Sandia National Laboratories

SANDIA REPORT
SAND2020-4284
Unclassified Unlimited Release
Printed April 2020

Prototype for Unclassified Radioisotope Algorithm

Eduardo A Padilla
Jesus J Valencia
Michael Higgins
Brian C Molley
Michael J Tanguay

Prepared by
Sandia National Laboratories
Albuquerque, New Mexico
87185 and Livermore,
California 94550

Issued by Sandia National Laboratories, operated for the United States Department of Energy by National Technology & Engineering Solutions of Sandia, LLC.

Available to DOE and DOE contractors from
U.S. Department of Energy
Office of Scientific and Technical Information
P.O. Box 62
Oak Ridge, TN 37831

Telephone: (865) 576-8401
Facsimile: (865) 576-5728
E-Mail: reports@osti.gov
Online ordering: http://www.osti.gov/scitech

Available to the public from
U.S. Department of Commerce
National Technical Information Service
5301 Shawnee Rd
Alexandria, VA 22312

Telephone: (800) 553-6847
Facsimile: (703) 605-6900
E-Mail: orders@ntis.gov
Online order: https://classic.ntis.gov/help/order-methods/

ABSTRACT

Continuing previous efforts to investigate and develop the Unclassified Radioisotope Algorithm, the goal of the FY19-FY20 effort was to develop a prototype detector system which uses the algorithm to confirm warhead attributes related to the presence of either weapons grade plutonium (WGPu) or highly enriched uranium (HEU). The final deliverable is a prototype attribute measurement system built with common, commercially available gamma radiation detector components, capable of confirming the presence of specific, complex radioactive sources of interest, without the collection and storage of gamma energy spectra. This is accomplished by processing each gamma pulse as it is received, applying weight values based on the energy and incrementing or decrementing scalar counters which can be compared with expected values to determine if the measured source is consistent with WGPu or HEU. This report documents the design of the prototype system as well as the development of the algorithm and performance testing results. While the previously conceptualized, simple algorithm resulted in a prohibitive amount of false positives, the goal for a simple attribute measurement system capable of verifying Ba-133 and Ra-226 (weapons grade plutonium and highly enriched uranium surrogate testing sources) at over 95% accuracy with sub 5% false positive rate was demonstrated.

Key words: Arms Control, Treaty Verification, Radiation Detection, Information Barrier, Attribute Measurement, Warhead Verification

ACRONYMS AND DEFINITIONS

Abbreviation	Definition
CsI	Cesium Iodide
DU	Depleted Uranium
FPGA	Field Programmable Gate Array
HEU	Highly Enriched Uranium
HPGe	High Purity Germanium
HV	High Voltage
MCA	Multi-channel Analyzer
NaI	Sodium Iodide
PMT	Photomultiplier Tube
PURA	Prototype for the Unclassified Radioisotope Algorithm
RGPu	Reactor Grade Plutonium
SiPM	Silicon Photomultiplier
SNM	Special Nuclear Material
WGPu	Weapons Grade Plutonium

CONTENTS

LIST OF FIGURES

LIST OF TABLES

1. INTRODUCTION

Continuing previous efforts to investigate and develop the Unclassified Radioisotope Algorithm, the goal of work in FY19 and early FY20 was to develop a prototype detector system which uses the algorithm to confirm warhead attributes related to the presence of either weapons grade plutonium (WGPu) or highly enriched uranium (HEU). The prototype attribute measurement system is built with common, commercially available gamma radiation detector components, capable of confirming the presence of specific, complex radioactive sources of interest, without the collection and storage of gamma energy spectra. This is accomplished by processing each gamma pulse as it is received, applying weight values based on the energy of the pulse, and incrementing or decrementing scalar counters. At the conclusion of the measurement, the tally in the scalar counters is compared with thresholds to determine if the measured source is consistent with WGPu or HEU. This report documents the design of the prototype system as well as the development of the algorithm and performance testing results.

1.1. Motivation

Under previous funding from the DOE/NNSA Office of Nuclear Verification (NA-243), Sandia National Laboratories developed the Unclassified Radioisotope Discrimination Algorithm as a proof of concept for an authenticatable and certifiable algorithm for discriminating weapons grade plutonium from other surrogate materials such as reactor grade plutonium and various radioactive sources such as Ba-133 and Am-241. Initially tested against simulated, non-classified sources of interest using a previously acquired high purity germanium (HPGe) detector response function, the proof of concept performed extremely effectively [1,2]. Continued efforts in FY18 using other sources of interest with low resolution detectors (NaI) have also bolstered the concept [3].

The primary motivation for this FY19 effort was to build a prototype system capable of demonstrating the performance and utility of the Prototype for Unclassified Radioisotope Algorithm (PURA). By building and testing PURA, this concept has proven its feasibility for use as an attribute measurement system in an arms control treaty verification scenario. Although the commercial hardware selected for the prototype was not intended for authentication, the underlying algorithm was designed to be suitable for authentication and certification by a host party; *at no point is a potentially classified gamma spectrum collected, stored or processed.*

1.2. Project Scope

As an initial prototype intended to demonstrate the feasibility of the algorithm, the development of the prototype followed a relatively simple development process. Designing the system for authentication and certification, inspectability, or tamper protection, was out of scope for the FY19 work beyond the inherent information protection provided by the algorithm itself. To allow for authentication and certification, it is anticipated that future versions will leverage the lower-level custom design aspects from 3G-TRIS and other efforts (e.g., SiPM readout, microprocessor/FPGA processing, and a simplified, authenticatable user input/control interface).

The prototype consists of a packaged digiBASE, Maestro software and Windows 10 PC used as a platform to develop the data acquisition and algorithm implementation processes.

The test and evaluation phase was designed to assess whether the algorithm, as implemented with an actual detector system, can confirm desired attributes with varying containerization (shielding) scenarios. In addition, the detector prototype was characterized to allow the algorithm to be assessed against simulated classified sources in future studies.

2. SYSTEM DESCRIPTION

This section provides an overview of the system architecture, including hardware design, system diagram and software design with algorithm implementation. As a demonstration prototype with technology readiness level (TRL) of four, the system prototype is capable of demonstration in a typical arms control verification environment such as a storage vault or highbay facility (i.e. – no environmental ruggedization has been developed.)

2.1. Hardware Design

The prototype system described here includes the following major components:

- 2" x 2" cylindrical CsI(Na) scintillator coupled to ruggedized 2" diameter photomultiplier tube (PMT)
- Industrial Windows 10 computer with integrated touch screen
- Ortec digiBASE high voltage (HV) power supply and multi-channel analyzer (MCA) tube base
- Power supply
- System enclosure

Figure 1 shows the high-level functional diagram for the system. This system collects pulse-by-pulse list mode data (pulse height and event time) through the digiBASE USB interface, which is then processed by the PURA algorithm (Section 2.2) on the PC. This data may be displayed on the integrated touch screen or on an external monitor for bench testing. All components are contained within a COTS enclosure for packaging and mobility. Algorithm outputs are displayed on the integrated display.

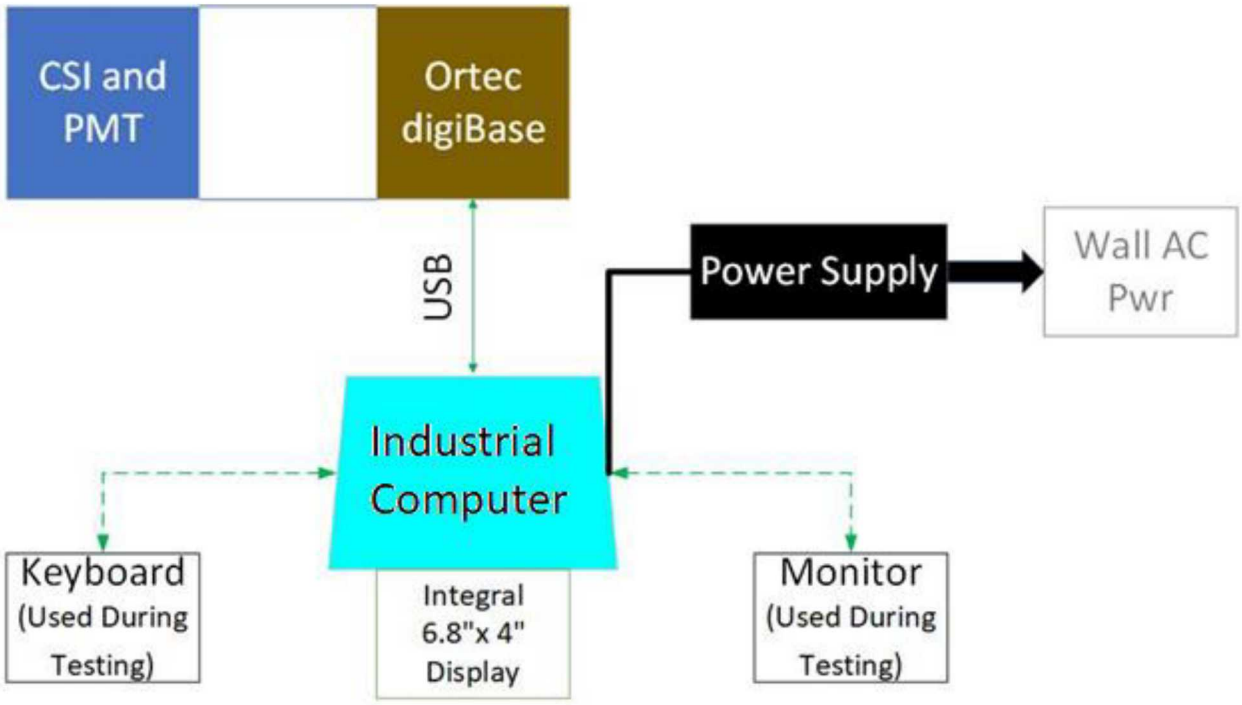

Figure 1 - High-level System Functional Diagram

The fully assembled PURA concept hardware is shown in Figure 2 below, performing a measurement of a source behind aluminum shielding.

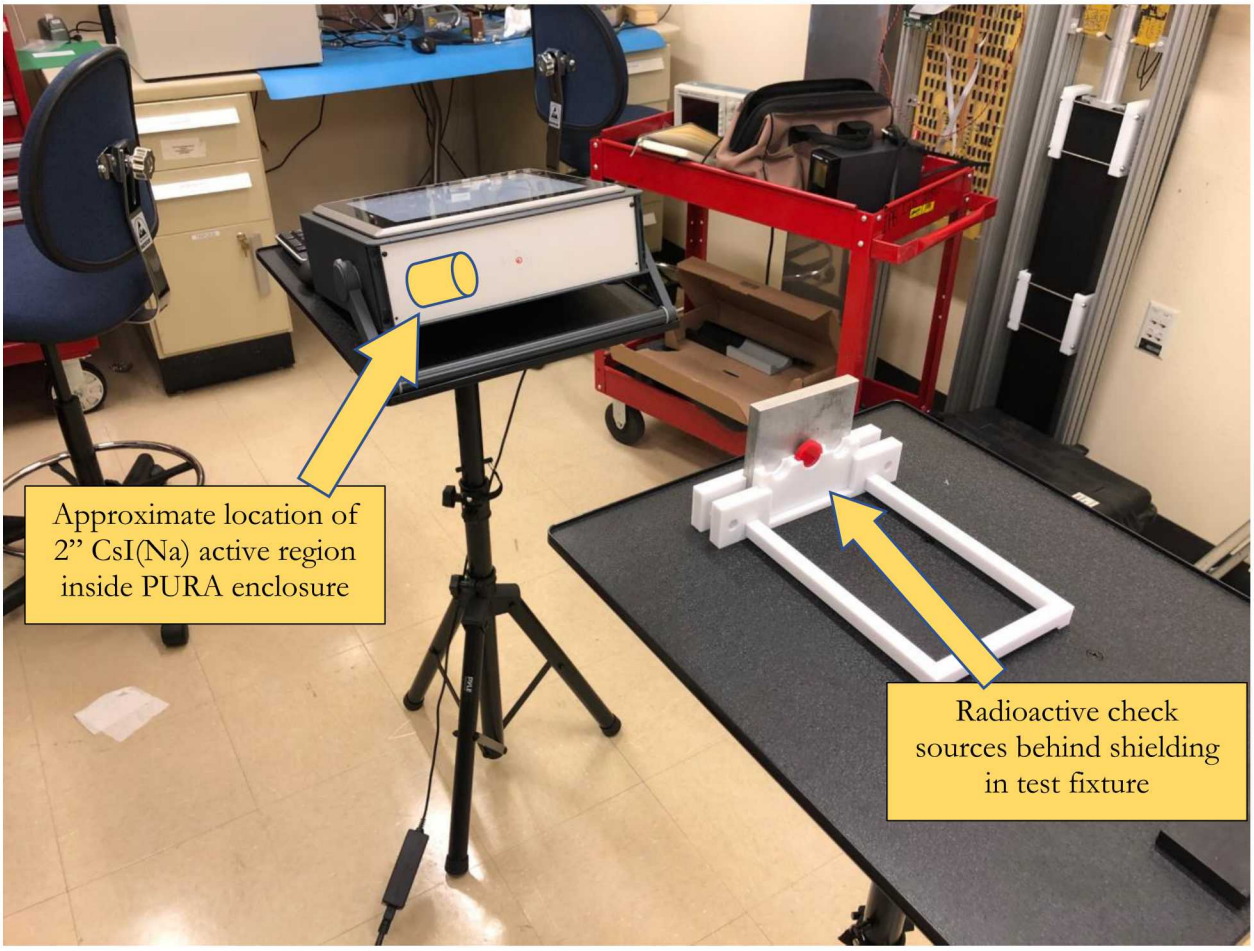

Figure 2 - PURA Prototype Measurement Configuration

A more detailed explanation of the prototype can be found in the Conceptual Design Document [4]. Minor changes from the conceptual design originally presented include a different industrial PC and associated enclosure due to availability of hardware from US vendors.

To enable repeatable and consistent testing with check sources, a small test fixture was created to secure the source and shielding plates during measurements (shown in white in Figure 2).

2.2. Software Design

The PURA software code is comprised of a C# Graphical User Interface (GUI) frontend (Figure 3), with C++ device interface code running in the backend. The backend code communicates with and controls the ORTEC digiBASE, from initializing detector settings, to collecting list mode data and running it through the algorithm.

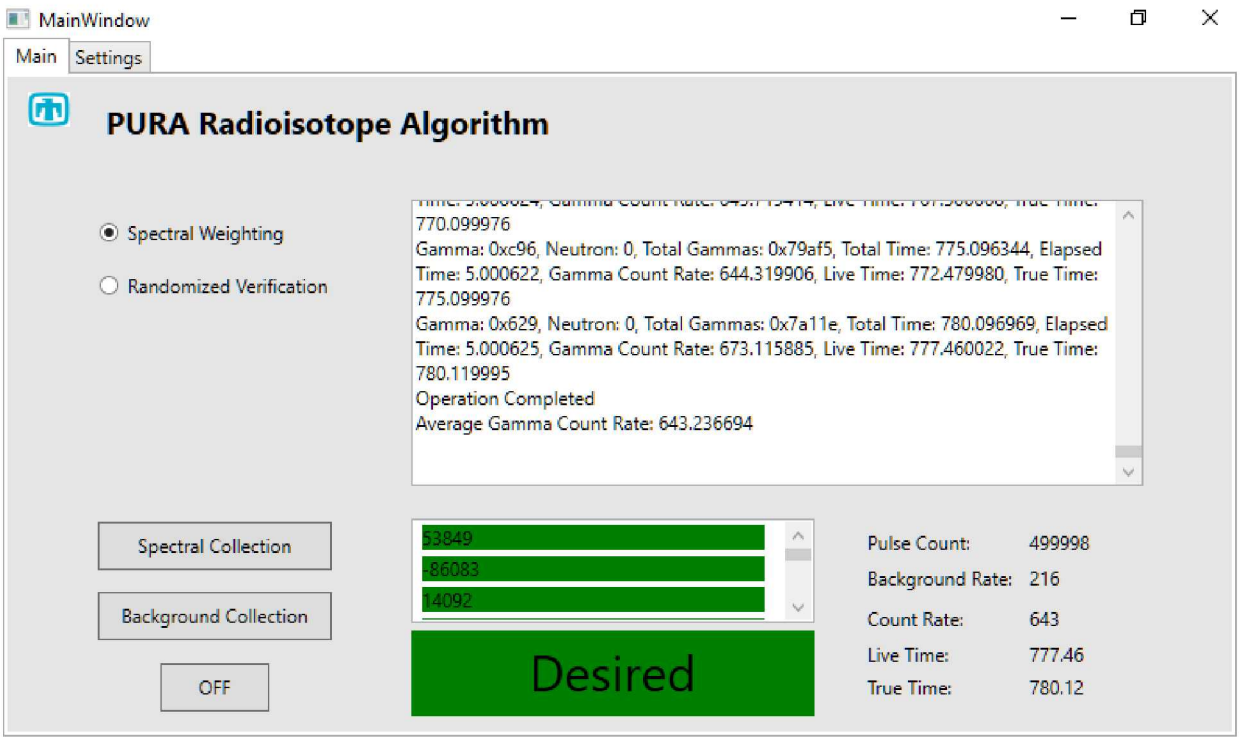

Figure 3 - PURA Graphical User Interface

Currently, the software is configured in a "debug" mode which displays more information than ultimately intended for a treaty verification scenario. Future versions of the GUI will only contain limited control options and restricted results display (count rate, red light/green light, heartbeat, etc.) for the inspectors. Further, the button labeled, "Spectral Collection" will be modified to read "Foreground Collection" as no spectrum is ever collected.

2.3. Algorithm Description

As described in the SAND reports listed in References [1-3], this system will measure the gamma radiation from an object of interest, pulse by pulse, and calculate multiple scalar values from previously constructed weight arrays. There are two primary modes of operation: Spectral Weighting and Randomized Verification. For Spectral Weighting, if the scalar weight value is consistent with that expected from a desired source of interest, the inspector will receive confirmation of the presence of that source. If not, a message will indicate no match. Randomized Verification uses a randomized weighting array and allows the inspector to create a "golden copy" template, which is then used to compare to subsequent treaty items without knowing the isotopic composition of the treaty accountable object.

The steps outlined below describe the high-level algorithm procedure:

1. A primary assumption is that detector has been calibrated manually. This means that any prototype system will need to be able to run Maestro via Windows upon power up and ensure that the detector has appropriate bias and gain settings.
2. The user will select "Background Count Rate" to measure ambient gamma radiation for 2 minutes, establishing a background count rate. This background count rate is used to

compare against the source measurement count rates to ensure a source strength of at least 3σ above background is being analyzed.

3. The user will select one of the two modes of operation described in the following two sections.
4. Each mode will have a single button to "Start Measurement".
5. Currently, the display is programmed to always show the calculated count rate for both background and foreground measurements in counts/second.

2.3.1. Spectral Weighting

1. Prior to use, all weight arrays (described in Section 3.3) will have been uploaded to memory for pulse comparison and weighting.
2. For each weight array, a dedicated tally counter keeps a running tally of each incoming gamma pulse weight value. Each weight array has an associated threshold value for Desired and Undesired (described in Section 3.4). These tally counters are all initialized to zero before each measurement.
3. A global pulse counter is also initialized zero, and the algorithm will stop once 1 million pulses are counted (this is an adjustable parameter in debug mode for testing).
4. Once a measurement has begun, a running average count rate is displayed. The software has an adjustable parameter to ensure the count rate is between minimum and maximum values (i.e., not too low of count rate and not too high). The minimum count rate will be equal to the background count rate (collected above), plus 3 times the square root of the background count rate. The number of standard deviations above background can be adjusted, but a minimum value of 3 is suggested to ensure greater than 90% probability of detection. Measurements that do not meet the minimum count rate will result in a warning message to the operator and no results will be displayed.
5. The maximum count rate is set to 20,000 counts per second. Count rates outside this range will cause an error message to display and prevent the algorithm from running. This limit can be adjustable but is a guard against pulse pileup effects which can distort the measured pulse heights.
6. During the measurement acquisition in list mode, each incoming pulse height (channel number in the MCA) is converted to a -1, 0 or +1 according the respective weight arrays and the tally counter is incremented or decremented accordingly.
7. After the desired number of pulses are registered, the algorithm will go through each weight array comparison and determine if any of the tallied results exceed the associated threshold, corresponding to a highly correlated "Desired" match. If so, the output displays a green box around the results, and red if no desired matches.

2.3.2. Randomized Verification

1. For this operating mode, a weight array for 1024 channels is created with -1's, 0's and +1's assigned randomly assigned.

2. The user will push a button labeled “Acquire Baseline”. When pressed, it performs a count rate check as described above to ensure a radioactive source is present, but also displays the scalar weight value after 1,000,000 pulses are processed.

3. After acquiring a baseline (golden copy), the button will change to read “Acquire Comparison”, and the user will repeat step 2.

4. The two resultant tally count values are then compared, and a “Pass” is given if the comparison value is within +/- 1 square root of the baseline counter value.

5. Both values are displayed and a green (Pass) or red (Fail) box appears.

3. TEST DESCRIPTION

The primary objective of this test and evaluation campaign is to ensure that the PURA prototype is capable of its proposed function: verifying the presence of WGPu and/or HEU. The project constraints preclude testing PURA with actual sources of WGPu and HEU for FY19. Therefore, the purpose of this effort is twofold: Collect sufficient characterization data to enable analytical performance evaluation against simulated WGPu and HEU sources, and test the PURA concept with actual measurement scenarios using surrogate sources to validate simulated performance.

Full detector characterization measurements were performed to enable the development of an accurate detector response function using GADRAS. This consisted of performing a series of characterization measurements at a fixed distance with various 10μCi check sources (Ba-133, Co-57, Co-60, Cd-109, Cs-137, Mn-54 and Na-22). With an accurate detector response function, high fidelity models can be rendered using GADRAS to simulate the response of the system to nearly any imaginable radioactive source such as those described in the final FY18 PURA report [3].

Additionally, to serve as model validation and physical confirmation of the analytical evaluation described in Section 4, a series of test measurements exercising the PURA concept were conducted. These tests included combinations of 10μCi surrogate test sources as described in Table 3-1 below. Due to the availability of low activity sources, the measurement times required to achieve 1 Million pulses were hours long, thus limiting the number of useful measurements we were able to collect.

Table 3-1 - Experimental Validation Data

Source
Ba-133 with ½" Al Shielding
Ba-133 + Co-60
Ba-133 + Na-22
Ba-133 + Ra-226
Ra-226 + Co-60
Ra-226 + Cs-137
Ra-226 + Mn-54

3.1. Source Selection

Actual measurements were performed with various low-strength (10μCi) gamma check sources described below. Simulated measurements were generated with source strengths of 10μCi, 100μCi, 200μCi, 350μCi, 500μCi, 750μCi and 1mCi for each isotope (desired and undesired) in order to support modeling validation over a range of count rates. As a surrogate source for WGPu and HEU, Ba-133 was selected for its various low-energy gamma lines (Figure 4) below approximately 600keV.

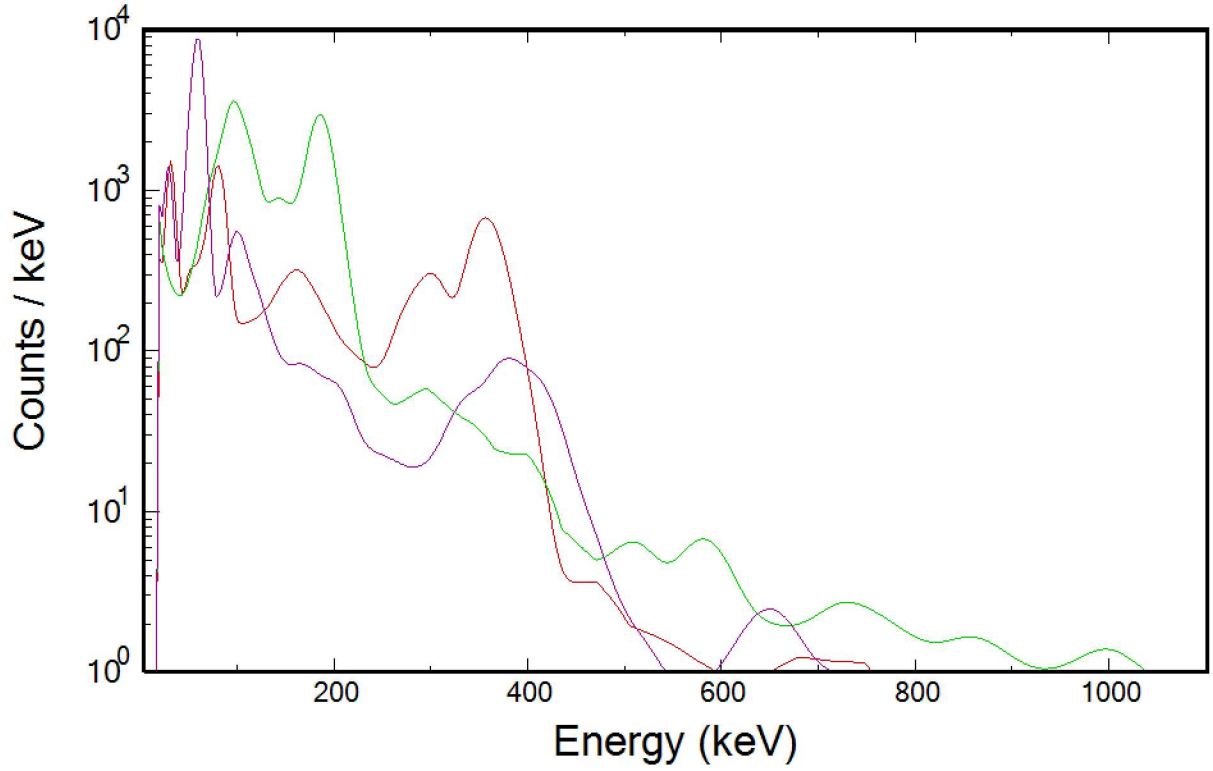

Figure 4 - Ba-133 (Red) vs. WGPu (Purple) and HEU (Green) Spectra

As a surrogate source for radioactive material containing higher energy gamma emissions such as thorium or uranium, Ra-226 was selected as a desired source (Figure 5). Although U-232 or Th-232 might serve as a better surrogate, Ra-226 was readily available for measurements.

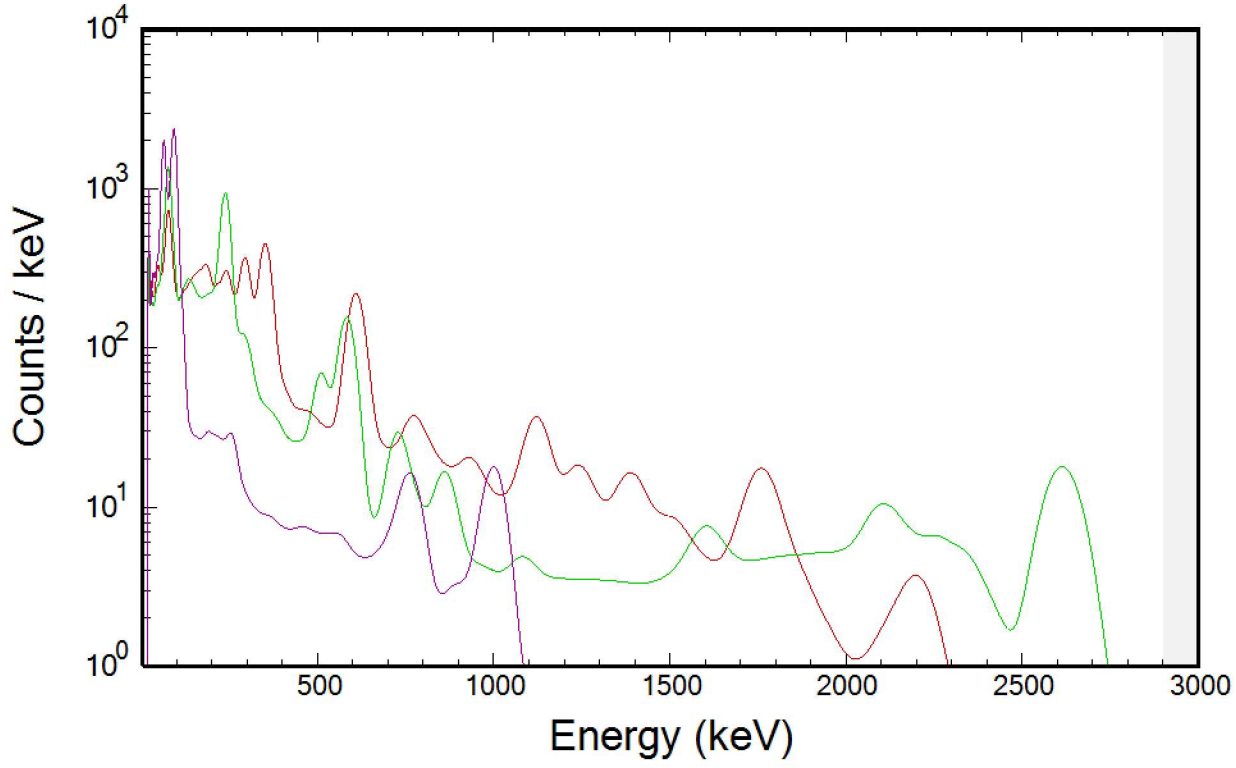

Figure 5 - Ra-226 (Red) vs. U-232 (Green) and U-238 (Purple)

Other readily available undesired sources used in testing and simulation included: Cd-109, Cs-137, Co-57, Co-60, Na-22 and Mn-54 (Figure 6.)

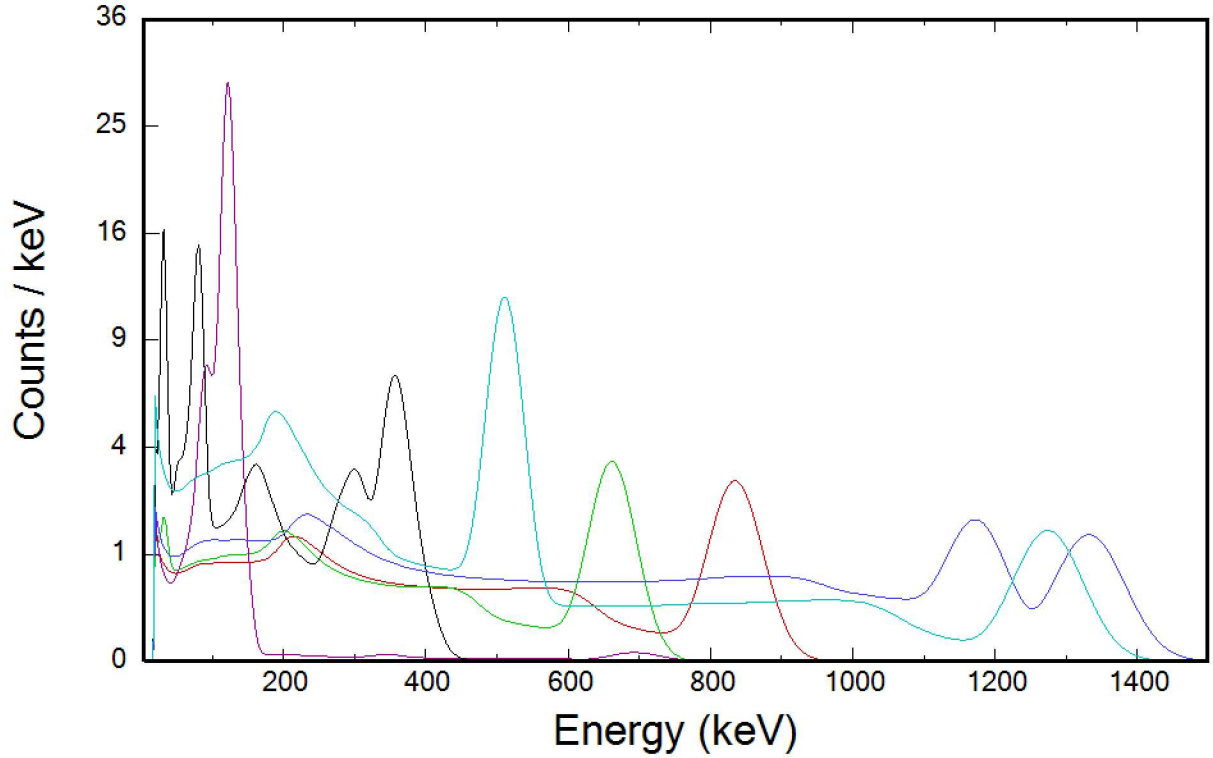

Figure 6 - Ba-133 (Black) Mn-54 (Red) Cs-137 (Green) Co-57(Purple) Co-60 (Blue) Na-22(Teal)

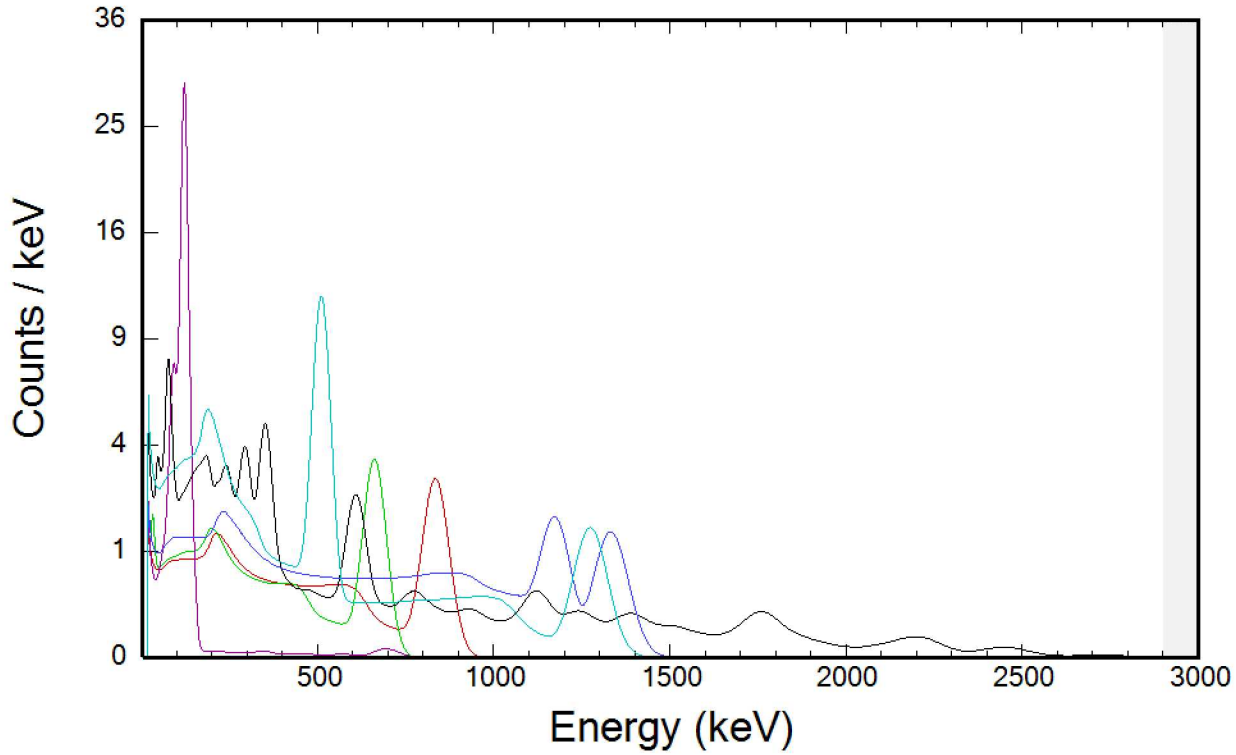

Figure 7 - Ra-226 (Black) Mn-54 (Red) Cs-137 (Green) Co-57(Purple) Co-60 (Blue) Na-22(Teal)

3.2. Shielding Selection

Several types of shielding material of varied thicknesses were originally planned for the measurement campaign. However, due to elevated background count rate and the availability of relatively low activity check sources, only a subset of thicknesses for Aluminum and Steel were tested, ranging from ¼" to 1" thick. It was not possible to obtain lead plates with requisite protective coatings before the end of FY19. 4" X 4" square plates were used in conjunction with the source test fixture show in Figure 2.

The figures below illustrate the expected relative count rates from a Ba-133 source versus thickness of aluminum, steel and lead shielding, respectively.

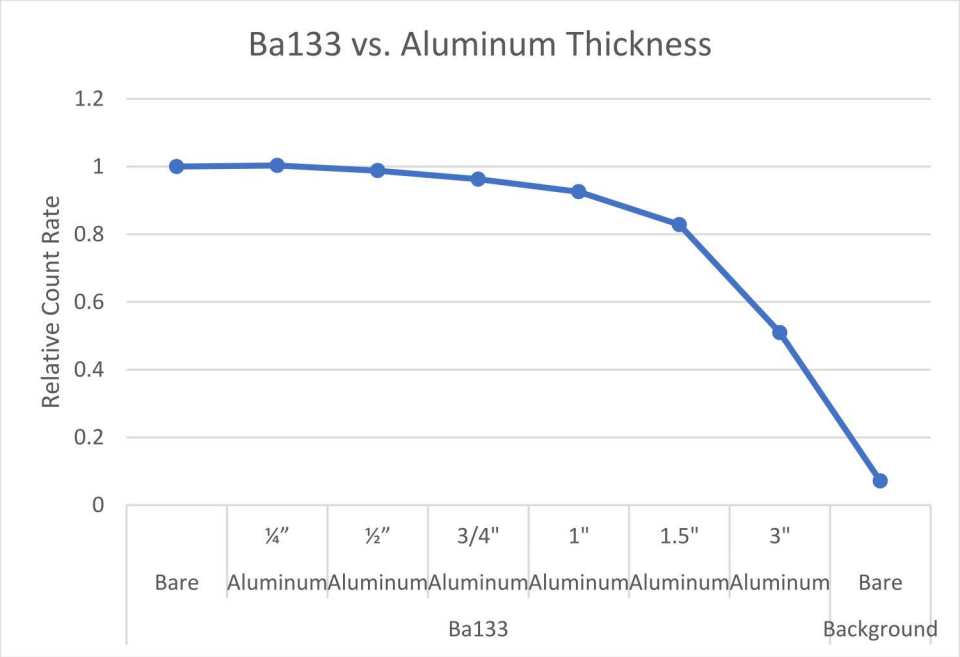

Figure 8 - Ba-133 Count Rate vs. Al Thickness

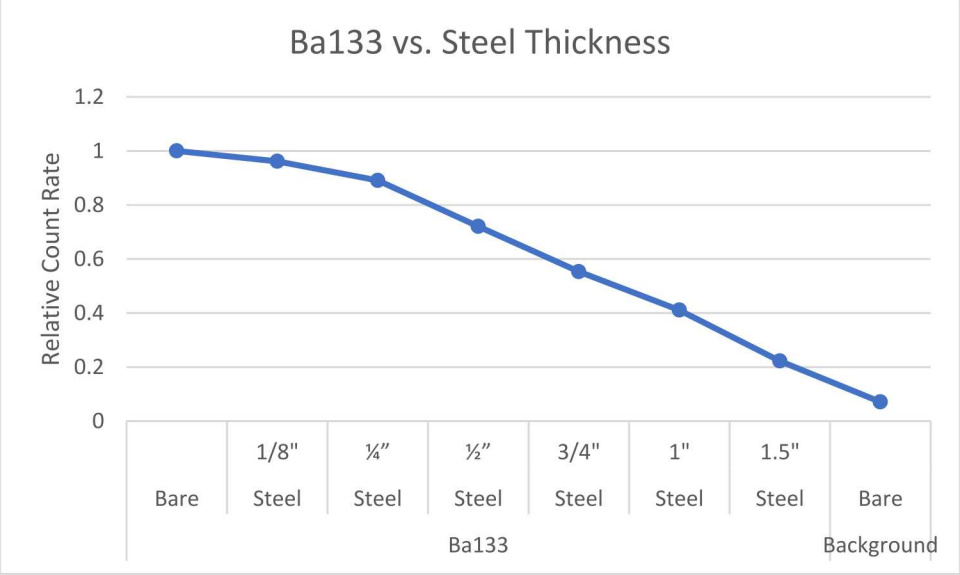

Figure 9 - Ba-133 Count Rate vs. Steel Thickness

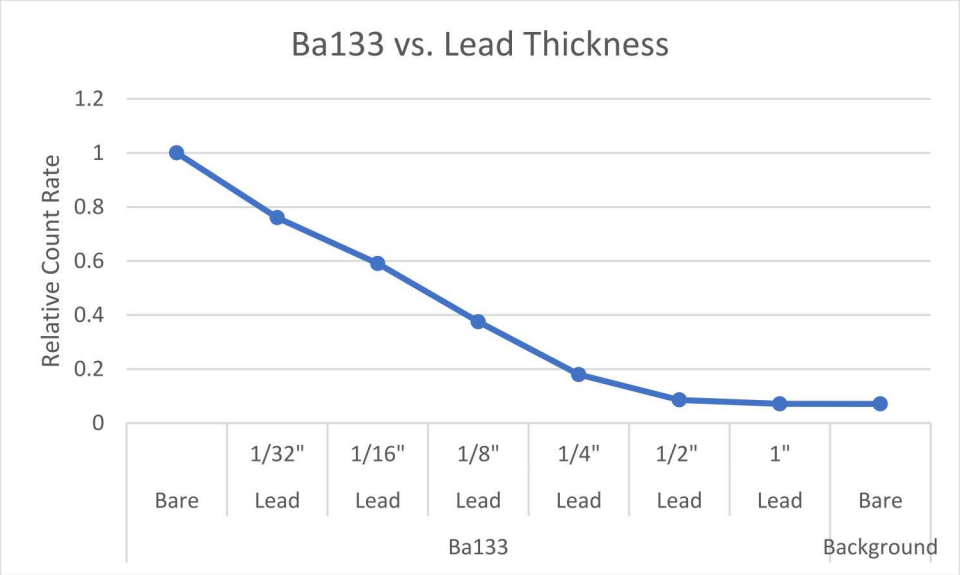

Figure 10 - Ba-133 Count Rate vs. Lead Thickness

The full list of shielding configurations used with each source in simulated calculations is shown in Appendix D.

3.3. Weight Array Generation

The initial weight generation process consisted of weighting simulated desired source spectra (Ba-133 and Ra-226 for this effort) against simulated undesired source spectra in multiple different shielding configurations at a fixed distance from the detector (Appendix D). Initially developed for a distance of 100cm, it was determined that the relatively low source strength of check sources and artificially high background count rate drove the decision to move the source distance to 50cm, defined as the distance from the face of the detector system to the center of the check source. Source models and simulated spectra were created in GADRAS, using a bare source configuration and shielding the source with various thicknesses of aluminum and steel. All spectra included a nominal source of natural background to reflect expected measurements.

Each ideal spectrum simulated in GADRAS was used as a Probability Density Function (PDF) to both generate ideal spectra containing exactly one million counts in the spectrum for the weight array generation process, as well as to sample from to generate realistic spectra with Poisson noise.

Once all the spectra were created, each desired source spectrum was paired with each undesired source spectrum for a total of 1,071 spectral pairs. From there, each channel (1024 channels total) in the spectral pair was assigned a weight of +1, 0, or -1. To determine weighting thresholds, the minimum count value for each channel in a spectral pair was used to determine if a significant difference exists (in that channel) between the two spectra. For example, if channel 10 in the undesired spectrum had 100 counts, and channel 10 in the desired channel had 120 counts, then the standard deviation (weight array sigma) was set to the square root of the minimum value (SQRT(100)=10). Since the difference in channel values was 20, this represents a two sigma difference with the desired spectrum having the larger count value in the bin. Therefore, a +1 would be assigned for channel 10 where the criteria for weight array optimization is one or two sigma. For larger sigma thresholds, this weight array channel would receive an importance of 0. The process is

identical if the undesired source channel value is larger, with a -1 value being assigned if the sigma threshold is met.

For this effort, we considered a number of weight array sigma thresholds, defined as multiples of the square root of the minimum count value for each channel in a spectral pair. A weight of +1 was assigned to any channel where the desired source counts were at least X sigma greater than the undesired source. Seven values of X used in this study were: 1, 2, 3, 5, 10, 20 and 40. A weight of -1 was assigned to channels where the undesired counts were at least X sigma greater than the desired counts. Any other channel was assigned a weight of 0.

Using the method described above, a total of seven different weight arrays were created for each desired-undesired spectral pair, resulting in a total of 214,131 individual weight arrays.

3.4. Resultant Value Threshold Optimization

Using the one million count ideal spectra generated previously, the dot product of each ideal spectrum (133 spectra for both Ba-133 and Ra-226 in this study) and each weight array was used to create a distribution of expected resultant scalar values for each weight array, and this was used to calculate the expected scalar value from measured data, plus or minus a given margin. This process overwhelmingly drives the ultimate performance of the algorithm.

Figure 9 and Figure 10 show example histograms of the distribution of the mean resultant scalar values, or mu (μ), as a function of sigma (σ) cut off values from the generation of weight arrays. Figure 9 shows a typical distribution of the 133 Ba-133 spectra against a single undesired spectrum weight array, with the shape of the distribution being consistent for the various pairwise weight arrays. However, the μ values can shift along the x-axis, based on the associated weight array generated for the undesired spectral pair. In general, with increasing sigma cut-off, the mean of the distribution of μ values decreases; as increasing the cut-off causes more values within the weight arrays to become 0, lowering the overall score. By increasing the threshold for assigning +1 or -1 values to the weight array, the net effect is that you are essentially throwing away information (assigning zero importances) and the maximum expected resultant value is lowered. A key assumption is made that the distributions of these resultants are normal, allowing the mean and standard deviation of a normal population to be used in determining the accuracy of this model. This assumption may not in fact be valid; more input data is needed to make this determination.

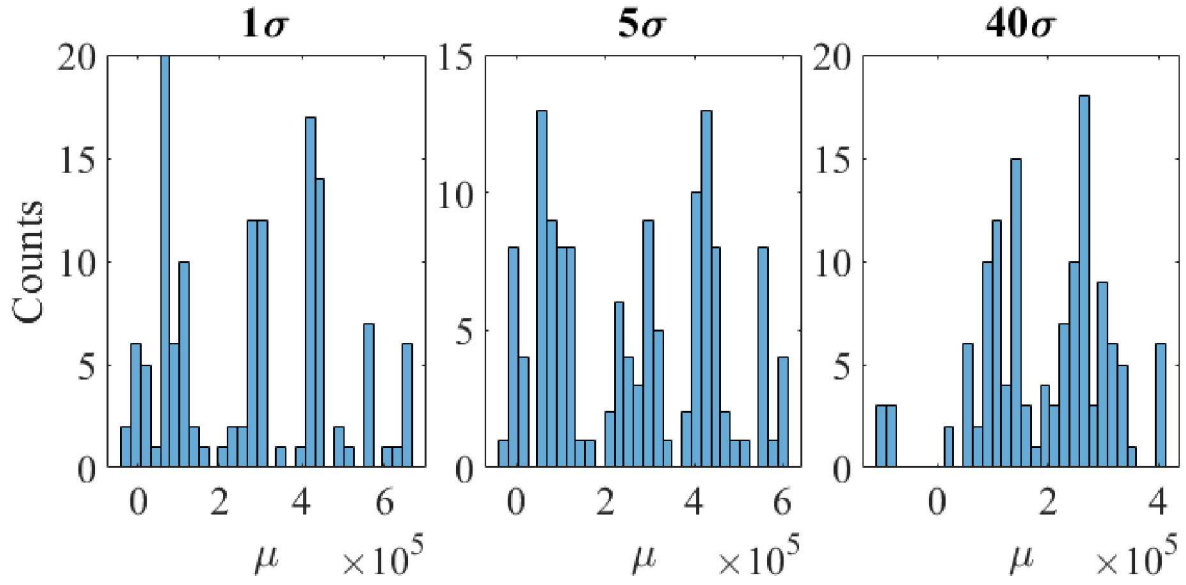

Figure 11 - Example Distribution of Ba-133 μ as a Function of σ Cutoff

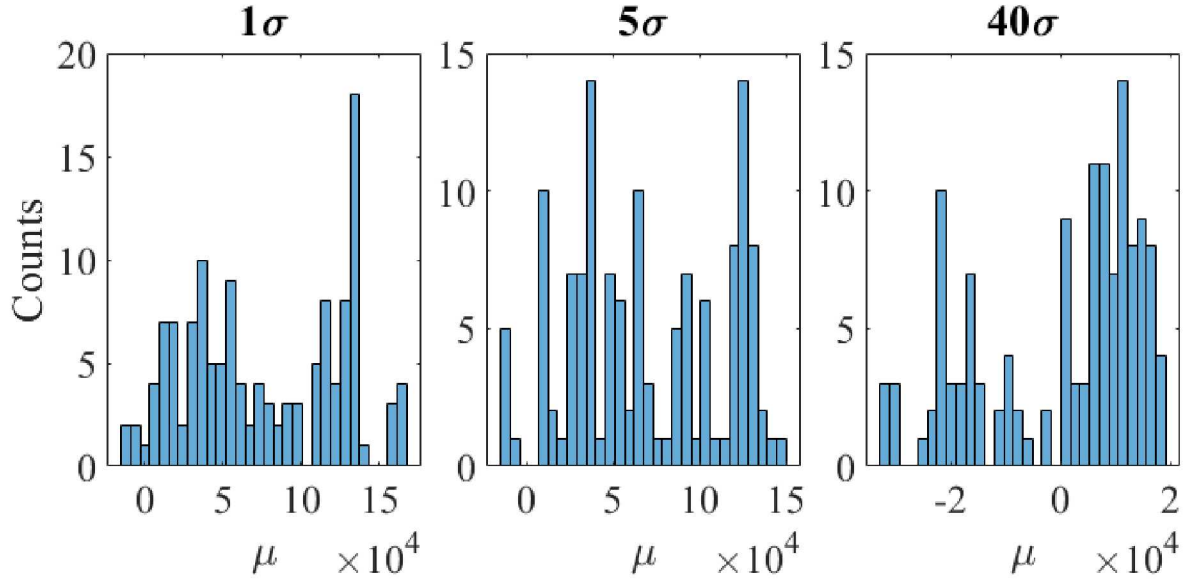

Figure 12 - Example Distribution of Ra-226 μ as a Function of σ Cutoff

Two approaches were tested in setting up upper and lower level discriminator (ULD/LLD) thresholds: the first is by implementing varied administrative limits on count rate for spectra to be run through the algorithm, the second is by changing the width of the ULD/LLD thresholds based on the standard deviation of the calculated normal populations.

In the first approach, all spectra below count rates at increasing multiples of the estimated background count rate (123 cps) were removed from the performance calculation process. This removal process was unbiased towards desired or undesired spectra. By removing spectra with lower

counts, as a ratio of the background count, it values the higher source strength sources in determining the mu and sigma values of the normal populations.

The second condition looked at the effect of changing the width of the discriminators. The ULD/LLD widths were investigated at 1 standard deviation of the normal population and 0.5 standard deviation of the normal population. The standard deviations were calculated for each undesired source spectrum with the assumption that the distribution of μ was normal (not necessarily valid as depicted in Figure 11 and Figure 12.) In this case the effect of decreasing the acceptable range for a positive identification was investigated on the effect of the accuracy of the system.

Along with the modelling of the bare and minimally shielded cases, 6 experimental bare conditions were compared to GADRAS data to see how the simulated data compared to the experimental data: 10μCi Ba-133, 10μCi Co-57, 10μCi Co-60, 10μCi Cs-137, 10μCi Na-22, and 10μCi Ra-226 were used. The algorithm is used to generate weight arrays for both the experimental and simulated data to see how the algorithm differentiated the two sets of data in terms of accuracy.

4. ANALYSIS OF RESULTS

Initially, the goal of this FY19 effort was to simply implement the algorithm described in Section 2.3. However, due to elevated background radiation levels and relatively weak test sources which challenged the performance of the system as designed, the focus of experimentation shifted to the optimization of algorithm parameters described in Section 3 above. Potential solutions to the issues encountered during the experimental portion of this project are described in Section 5 below.

The method of assessing the strength of this algorithm is based on the statistical derivation of accuracy described here. Following the generation of the weight arrays, the dot product of each spectra and weight array is calculated. The resultant dot product was placed into four statistical categories, based on if it is a desired or undesired spectrum, and if the value falls between the upper and lower limit discriminators (calculated based on the standard deviation of the distribution of desired spectra resultants.) The four statistical categories were true positives (TPs), false positives (FPs), true negatives (TNs), and false negatives (FNs). These four categories determine how well the algorithm worked at determining if a radioactive source could be categorized as desired or undesired without storing and processing a gamma ray spectrum.

Depending on the count rate thresholds and weight array optimization sigma cut-off values, the algorithm ran spectra through all relevant weight arrays and determined three key attributes: accuracy, defined as the total TPs and TNs over the sum of all statistical categories, false positive rate (FPR) defined as the total FPs over the sum of TNs and FPs, and the true positive rate (TPR) defined as the total TPs over the sum of TPs and FNs. Utilizing the accuracy, FPR, and TPR, an understanding of where the model excels was further understood.

4.1. Experimental Results

Initial testing with the sources described in Section 3.1 and the algorithm as described in Section 2.3 was not successful. Originally, the false positive rate was expected to be much lower, thus enabling a mode of operation which would indicate the presence of Ba-133/Ra-226 if any of the thousands of weight array thresholds were met. However, the unexpectedly high false positive rate resulted in each measurement positively indicating the presence of Ba-133/Ra-226. This required a shift in the focus of testing towards statistical analyses of an expanded number of weight array comparisons using simulated data.

Several long duration measurements collecting list-mode data were performed to serve as model validation. The following figures show three experimental and three simulated spectra. The grouping of spectra with yellow/reddish coloring is measured data, while the grouping of spectra with the green/blueish coloring is simulated data. Two notable discrepancies are illustrated in the data: a slight detector gain offset and increased background radiation in the measured data. The detector gain offset is attributable to a simple error in detector gain settings during the measurements (compared to the initial settings used when characterizing the detector in GADRAS). It is not expected that this slight gain offset is very significant. Additionally, the measured background radiation level is higher than normally encountered in Albuquerque due to myriad sources present in our lab at the time of testing. This likely hindered performance slightly, but does not invalidate the model results as a typical background source definition for Albuquerque was used in the models.

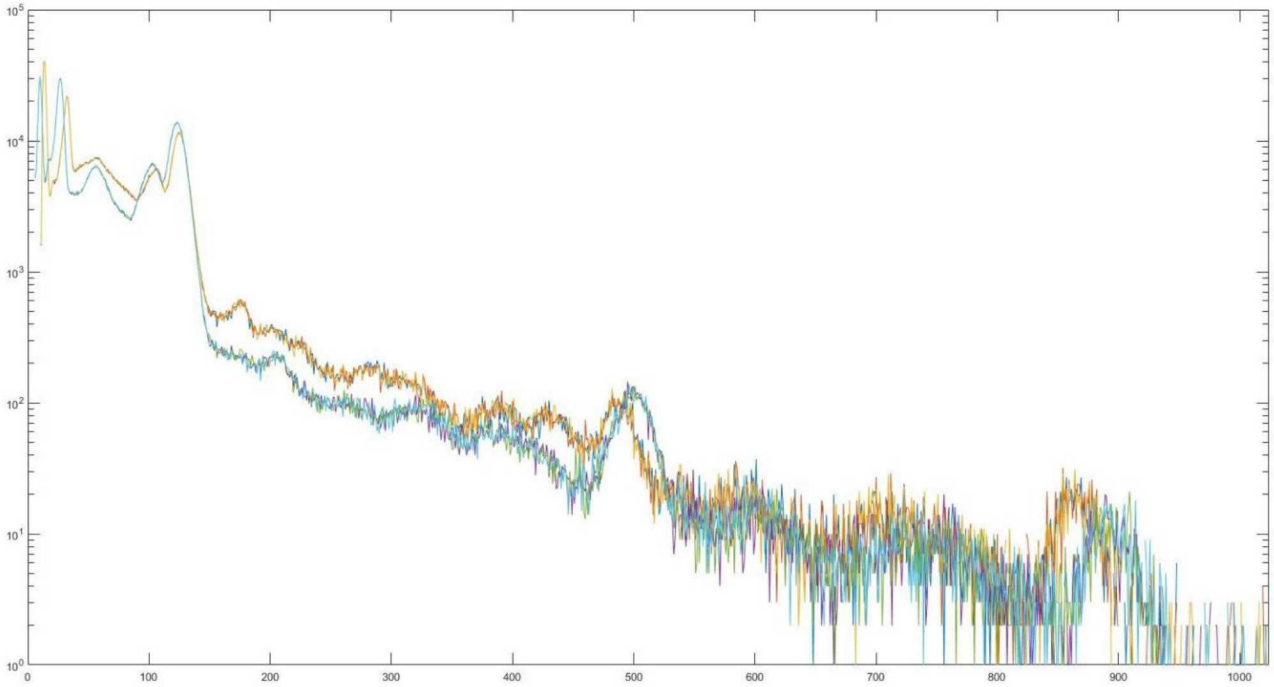

Figure 13 - Experimental vs. Simulated Ba-133 Spectra

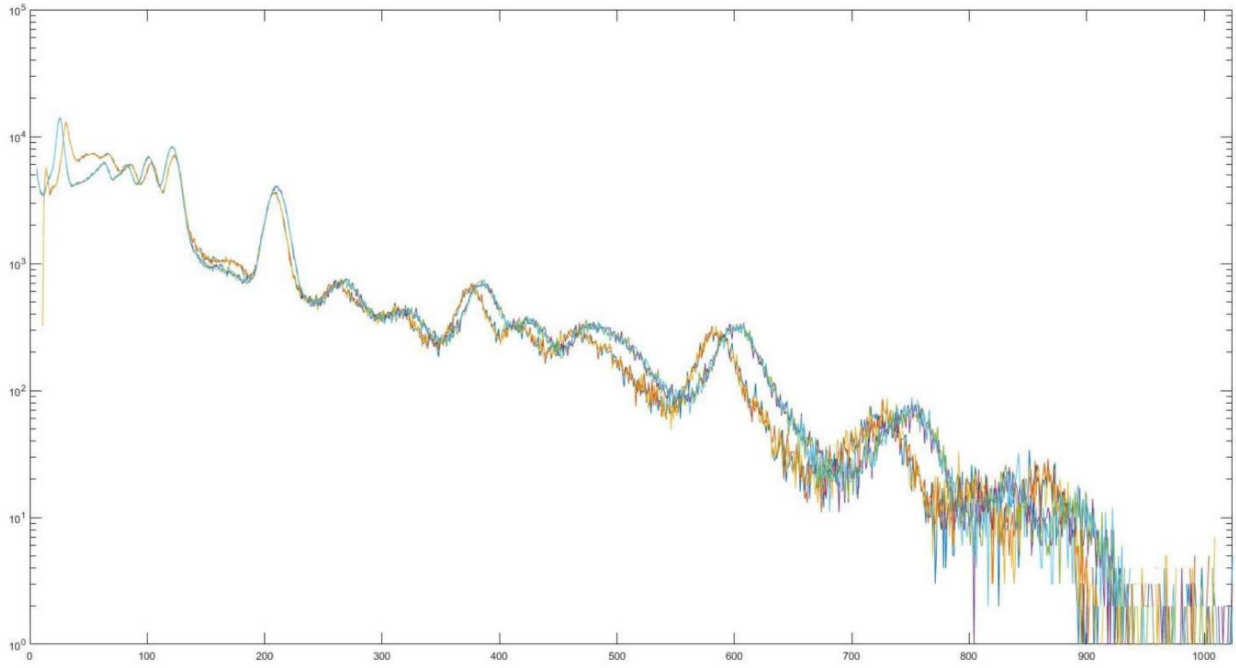

Figure 14 - Experimental vs. Simulated Ra-226 Spectra

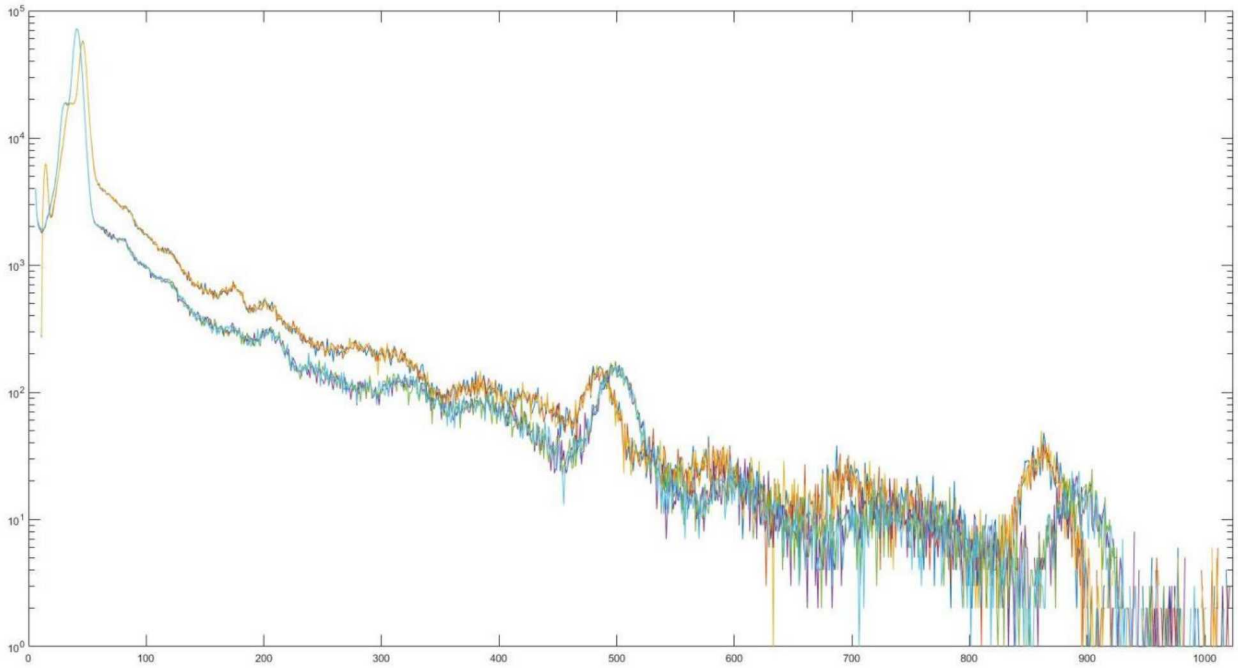

Figure 15 - Experimental vs. Simulated Co-57 Spectra

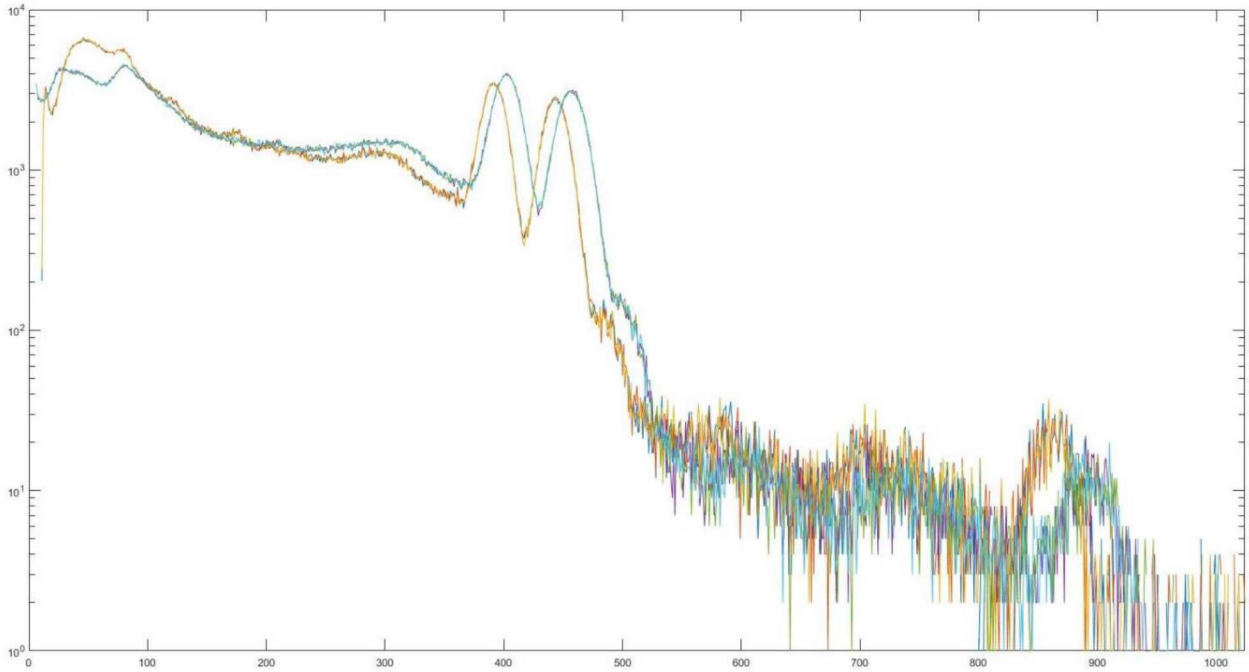

Figure 16 - Experimental vs. Simulated Co-60 Spectra

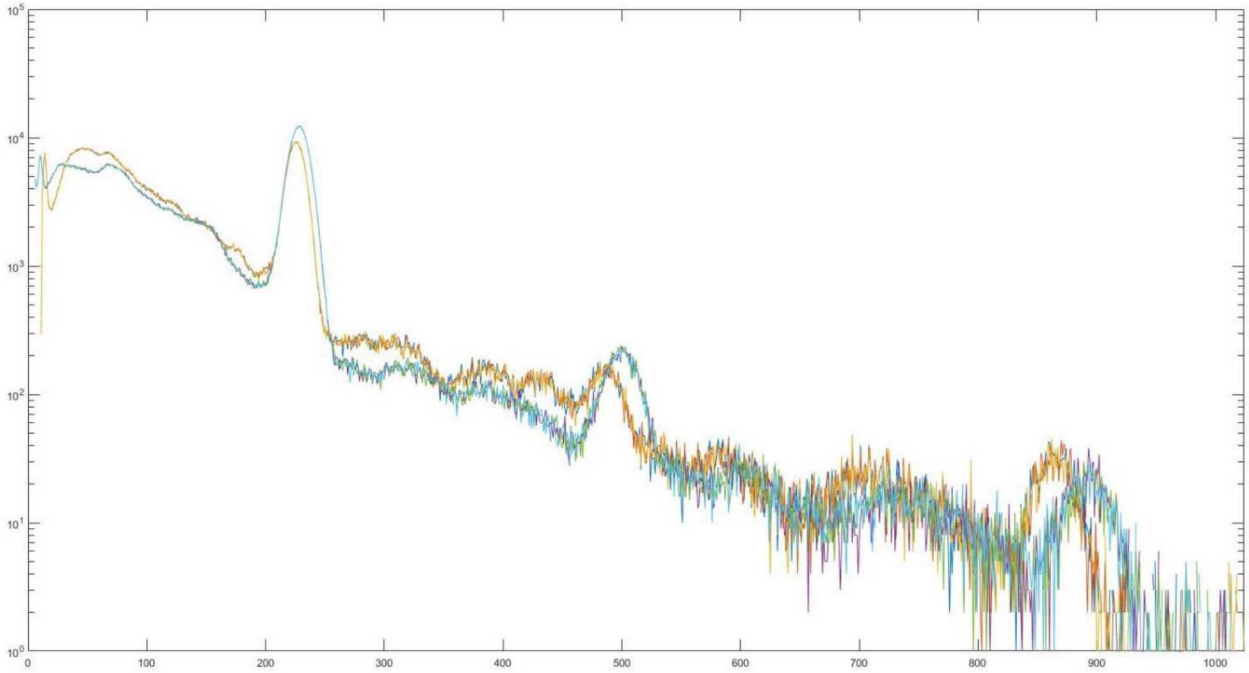

Figure 17 - Experimental vs. Simulated Cs-137 Spectra

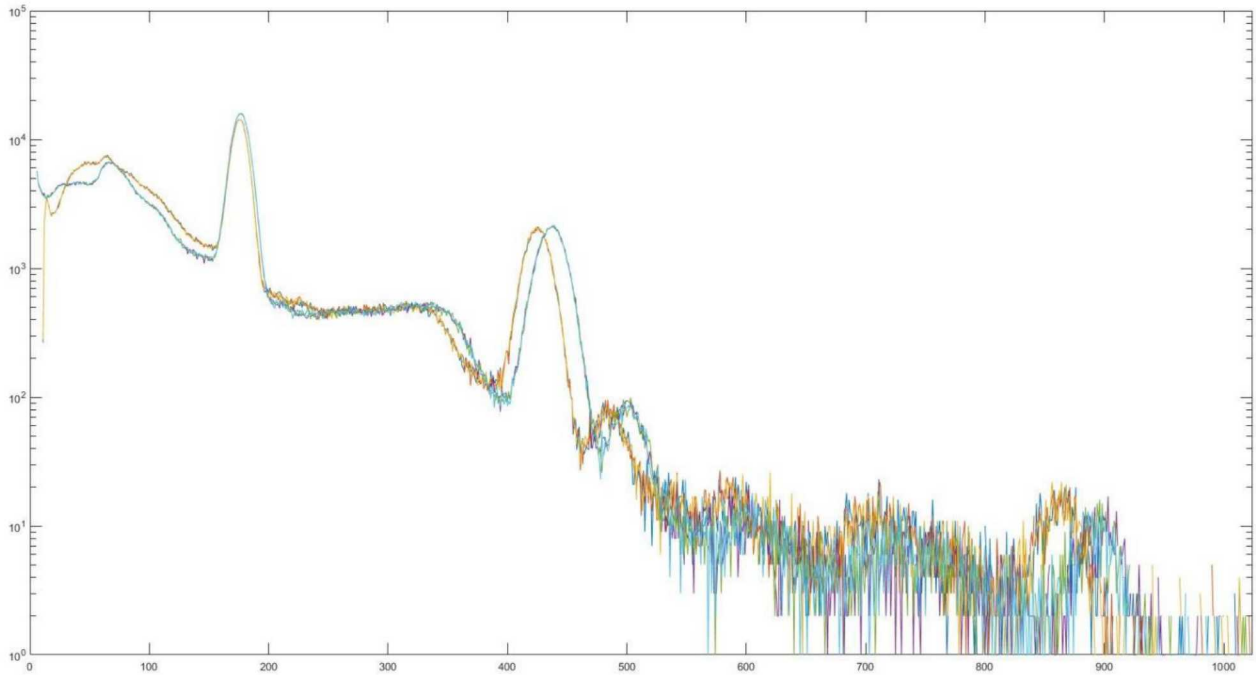

Figure 18 - Experimental vs. Simulated Na-22 Spectra

The following table summarizes the performance of the six (total) spectra when run through over 32,000 one sigma optimized weight arrays. The weight arrays were optimized based on simulated data, therefore this partly explains the slightly improved performance compared to measured data with a small calibration offset. Additionally, the higher background count rate in the lab likely diminished performance. However, the overall accuracy and true positive rates are in close agreement for both Ba-133 and Ra-226.

Table 4-1 - Experimental versus Simulated Results

	Accuracy	FPR	TPR
Measured Ba-133	77%	21.0%	63.7%
Simulated Ba-133	83%	12.5%	63.7%
Measured Ra-226	72%	21.0%	14.8%
Simulated Ra-226	72%	12.5%	9.8%

4.2. Simulated Results

In the case of the baseline data of 1071 spectra, a total of 214,130 weight arrays were generated, with 107,605 individual weight arrays for both Ba-133 and Ra-226. Each spectrum (no count rate limitations) was run through all 214,130 weight arrays to characterize the statistical performance of the algorithm. Table 4-2 lists the overall results for Ba-133 and Table 4-3 lists the overall results for the Ra-226 data.

Table 4-2 - Ba-133 Statistical Results as a Function of Weight Array Sigma

	Accuracy	FPR	TPR
One Sigma	90%	7.2%	72.9%
Two Sigma	90%	7.4%	72.9%
Three Sigma	90%	7.6%	72.8%
Five Sigma	90%	7.6%	72.7%
Ten Sigma	90%	7.3%	72.4%
Twenty Sigma	91%	6.7%	72.3%
Forty Sigma	91%	6.7%	71.3%

Table 4-3 - Ra-226 Statistical Results as a Function of Weight Array Sigma

	Accuracy	FPR	TPR
One Sigma	66%	26.3%	15.3%
Two Sigma	66%	26.4%	15.3%
Three Sigma	66%	26.5%	15.3%
Five Sigma	66%	26.9%	15.2%
Ten Sigma	65%	27.9%	15.2%
Twenty Sigma	63%	30.8%	15.8%
Forty Sigma	58%	35.9%	17.1%

A key assumption of the algorithm is that every spectrum has 1 million counts and neglects the amount of time required for the million counts to occur. Because of this fact, certain spectra that have very low count rates can end up skewing the results of the algorithm. In order to test the effect of these low activity sources on the resultant, a background limiter is utilized to remove spectra that

have very low count rates. Increasing count rate limits were applied to test this effect; removing all spectra below the background count rate, 2 times the count rate, and so forth up to 100 times the baseline background count rate. This process increasingly removes the low activity and heavily shielded sources.

In both cases, optimal performance was noted while using one sigma optimized weight arrays. By lowering the threshold in which a +1 or -1 weight is applied is each channel, the corresponding resultant values contain more information (i.e. – there are less zero weighted channels). In removing spectra with lower count rates, this method benefitted Ba-133 while lowering the performance of Ra-226. This effect is likely due to the relatively high contribution of background radiation to the sub-500keV region of the energy spectrum where Ba-133 has many characteristic lines. However, with Ra-226 characteristic emissions having both higher and lower energy emissions, this effect negates itself. The full performance data is listed in Appendix B.

Optimal performance for Ba-133 was observed with one sigma weight array optimization and 100X count rate limits: 94% Accuracy, 5% false positive rate and 82% true positive rate. Under these conditions**, the algorithm produced the correct characterization of Ba-133 presence or absence 94% of the time**.

Optimal performance for Ra-226 was observed with one sigma weight array optimization and no count rate limits: 66% Accuracy, 26% false positive rate and 15% true positive rate.

Appendix B.1 shows all the confusion matrices for both Ba-133 and Ra-226.

4.3. Conclusions

It is clear from initial testing that the original, simple algorithm based on previously developed methods of weight array optimization is not feasible. While this approach is extremely effective at differentiating two specific sources of interest (Appendix C), attempting to apply it nakedly to a semi-infinite set of potential sources as an attribute measurement system results in poor performance. The possibility for a simple attribute verification implementation still exists, yet it will require further refinement of both the weight array optimization process, administrative and engineering controls and in-depth, realistic testing. The performance of the algorithm as it stands is largely driven by the ability to limit the variability of sources of interest.

However, the overall performance of the algorithm across thousands of individually optimized weight arrays shows tremendous promise. Further, there are many direct methods for refinement which have been identified throughout this process which promise to increase the performance to levels matching fully intrusive, expert gamma spectroscopic analysis. These methods for improvement are identified in Section 5. By adopting attribute verification thresholds based on an aggregation of a wide scale of statistics, a simple attribute measurement system capable of verifying the presence of weapons grade plutonium or highly enriched uranium at over 95% accuracy with sub 5% false positive rate is already proven, with a low-resolution CsI(Na) gamma detector. Appendix C shows expected performance improvements when comparing HPGe to NaI(Tl) detectors, and the addition of neutron information will further boost performance.

5. FUTURE WORK

With a functional prototype system for testing the PURA concept now complete, there is much work which remains to fully optimize the algorithm for given scenarios. The results presented in the previous section highlight the need for further refinement of the algorithm when applied to a broad scope of undesirable sources. This should be readily achievable through the investigation and application of methods involving further parametric optimization, dimensional reduction, incorporating neutron signatures and other hardware/system level changes.

5.1. Parametric Study

Now that a modeling and simulation platform has been created and benchmarked, much progress can be realized through the exploration, characterization and optimization of various expected signatures. More realistic sources of interest can be modeled in expected potential treaty verification geometries. This will help to determine the limits of performance for all types of sources and shielding scenarios. Additionally, as evidenced by the performance of Ra-226, a concept for energy efficiency weighting was conceived which can help account for the effective lack of signal at higher energies. By multiplying the optimized weight arrays by the detector's energy efficiency, the 1 million count spectra can effectively be "flattened" to better weight source emissions rather than detector efficiency and environmental scatter.

As this is fundamentally a classification problem, well developed techniques from machine learning classifiers such as TensorFlow can be leveraged to optimize the weight arrays for massive sets of sources of interest.

5.2. Dimensional Reduction

As a more deliberate method of parametric study, formal methods of dimensional reduction can be applied to limit the potentially infinite space of potential spoof sources. Such techniques which can be investigated include: low variance filtering, high correlation filtering, random forest, backward/forward feature elimination, principal component analysis and various projection based approaches.

5.3. Neutron Analysis

For enhanced performance in verifying the presence of plutonium or highly enriched uranium, neutron detection modalities can easily be added to weight arrays as independently weighted dimensions. This can range from neutron count rate (passive or active interrogation), to more advanced techniques such as multiplicity and neutron spectrum analysis.

5.4. System Modification

In parallel to analytical efforts, several ideas for system modification could be explored. The most likely impactful improvement can be achieved by selecting another detector type. High resolution spectroscopic gamma detectors such as HPGe, or even neutron sensitive CLLBC (Cs2LiLa(Br,Cl)6:Ce) detectors can be leveraged to increase the accuracy of the system. To help lower the signal to noise ratio, high density collimation can be implemented simply.

APPENDIX A. REFERENCES

[1] Kallenbach, Gene A., *Unclassified Radioisotope Discrimination FY2016 Final Report*, SAND2016-9031, Sandia National Laboratories, September 2016

[2] Kallenbach, Gene A., Hamel, Michael C., *Unclassified Radioisotope Discrimination Final Report*, SAND2018-0868, Sandia National Laboratories, January 2018

[3] Padilla, Eduardo A., Weber, Thomas M., Kallenbach, Gene A., Valencia, Jesus J., *Performance of Unclassified Radioisotope Algorithm FY2018 Year End Report*, SAND2018-12834, Sandia National Laboratories, October 2018

[4] Padilla, Eduardo A., Spiak, Stephen R., *Prototype for Unclassified Radioisotope Algorithm: Conceptual Design*, SAND2019-2345, Sandia National Laboratories, February 2019

APPENDIX B. PERFORMANCE DATA

The following tables list the confusion matrices for the various conditions tested in this project, either testing Ba-133 or Ra-226 as the desired source.

B.1. Confusion Matrices

Table B-1 - Ba-133 Statistical Results Based on Count Rate Removal and Weight Array Sigma

1 Sigma

	0 CR	3X CR	5X CR	10X CR	20X CR	35X CR	50X CR	75X CR	100X CR
TP	9%	11%	10%	11%	11%	10%	10%	10%	10%
FP	6%	6%	5%	4%	4%	4%	4%	4%	4%
TN	81%	81%	82%	82%	82%	83%	83%	84%	84%
FN	3%	3%	3%	3%	3%	3%	3%	2%	2%
Accuracy	90%	92%	92%	93%	93%	93%	93%	93%	94%
FPR	7%	6%	6%	5%	5%	5%	5%	5%	5%
TR	73%	80%	78%	78%	79%	79%	80%	81%	82%

2 Sigma

	0 CR	3X CR	5X CR	10X CR	20X CR	35X CR	50X CR	75X CR	100X CR
TP	9%	11%	10%	11%	11%	10%	10%	10%	10%
FP	7%	6%	5%	5%	5%	5%	4%	5%	4%
TN	81%	81%	82%	82%	82%	83%	83%	83%	83%
FN	3%	3%	3%	3%	3%	3%	3%	2%	2%
Accuracy	90%	91%	92%	92%	92%	93%	93%	93%	93%
FPR	7%	7%	6%	6%	5%	5%	5%	5%	5%
TR	73%	80%	78%	78%	79%	79%	80%	81%	82%

3 Sigma

	0 CR	3X CR	5X CR	10X CR	20X CR	35X CR	50X CR	75X CR	100X CR
TP	9%	11%	10%	11%	11%	10%	10%	10%	10%
FP	7%	6%	5%	5%	5%	5%	5%	5%	5%
TN	81%	80%	81%	81%	82%	83%	83%	83%	83%
FN	3%	3%	3%	3%	3%	3%	3%	2%	2%
Accuracy	90%	91%	92%	92%	92%	93%	93%	93%	93%
FPR	8%	7%	6%	6%	6%	5%	5%	5%	5%
TR	73%	80%	78%	78%	79%	79%	80%	81%	82%

5 Sigma

	0 CR	3X CR	5X CR	10X CR	20X CR	35X CR	50X CR	75X CR	100X CR
TP	9%	11%	10%	11%	11%	10%	10%	10%	10%
FP	7%	6%	6%	5%	5%	5%	5%	5%	5%
TN	81%	80%	81%	81%	81%	82%	83%	83%	83%
FN	3%	3%	3%	3%	3%	3%	3%	2%	2%
Accuracy	90%	91%	91%	92%	92%	92%	93%	93%	93%
FPR	8%	7%	7%	6%	6%	6%	6%	6%	6%
TR	73%	79%	78%	78%	79%	79%	80%	81%	82%

10 Sigma

	0 CR	3X CR	5X CR	10X CR	20X CR	35X CR	50X CR	75X CR	100X CR
TP	9%	11%	10%	11%	11%	10%	10%	10%	10%
FP	6%	6%	5%	5%	5%	5%	5%	5%	5%
TN	81%	80%	81%	81%	82%	82%	83%	83%	83%
FN	3%	3%	3%	3%	3%	3%	3%	2%	2%
Accuracy	90%	91%	92%	92%	92%	92%	93%	93%	93%
FPR	7%	7%	6%	6%	6%	6%	6%	6%	5%
TR	72%	79%	78%	78%	78%	78%	80%	81%	82%

20 Sigma

	0 CR	3X CR	5X CR	10X CR	20X CR	35X CR	50X CR	75X CR	100X CR
TP	9%	11%	10%	11%	11%	10%	10%	10%	10%
FP	6%	5%	5%	5%	5%	5%	5%	5%	5%
TN	82%	81%	82%	82%	82%	83%	83%	83%	83%
FN	3%	3%	3%	3%	3%	3%	3%	2%	2%
Accuracy	91%	92%	92%	92%	92%	93%	93%	93%	93%
FPR	7%	6%	6%	6%	5%	5%	5%	5%	5%
TR	72%	79%	78%	77%	78%	79%	80%	81%	83%

40 Sigma

	0 CR	3X CR	5X CR	10X CR	20X CR	35X CR	50X CR	75X CR	100X CR
TP	9%	11%	10%	10%	10%	10%	10%	10%	10%
FP	6%	6%	6%	5%	5%	5%	5%	5%	5%
TN	82%	81%	81%	81%	81%	82%	82%	82%	83%
FN	4%	3%	3%	3%	3%	3%	3%	2%	2%
Accuracy	91%	91%	91%	91%	91%	92%	92%	92%	93%
FPR	7%	7%	6%	6%	6%	6%	6%	6%	6%
TR	71%	78%	76%	76%	77%	78%	79%	81%	82%

Table B-2 - Ra-226 Statistical Results Based on Count Rate Removal and Weight Array Sigma

1 Sigma

	0 CR	3X CR	5X CR	10X CR	20X CR	35X CR	50X CR	75X CR	100X CR
TP	2%	2%	2%	2%	2%	3%	2%	3%	3%
FP	23%	23%	23%	23%	23%	23%	24%	23%	23%
TN	65%	62%	61%	61%	60%	59%	59%	58%	57%
FN	11%	13%	13%	13%	14%	15%	15%	16%	17%
Accuracy	66%	64%	64%	64%	63%	61%	62%	60%	60%
FPR	26%	27%	27%	28%	28%	28%	29%	29%	29%
TR	15%	15%	15%	15%	15%	14%	14%	13%	13%

2 Sigma

	0 CR	3X CR	5X CR	10X CR	20X CR	35X CR	50X CR	75X CR	100X CR
TP	2%	2%	2%	2%	2%	3%	2%	3%	3%
FP	23%	23%	23%	23%	23%	23%	24%	23%	24%
TN	64%	62%	61%	61%	60%	59%	59%	58%	57%
FN	11%	13%	13%	13%	14%	15%	15%	16%	17%
Accuracy	66%	64%	64%	63%	63%	61%	62%	60%	60%
FPR	26%	27%	27%	28%	28%	29%	29%	29%	29%
TR	15%	15%	15%	15%	15%	14%	14%	13%	13%

3 Sigma

	0 CR	3X CR	5X CR	10X CR	20X CR	35X CR	50X CR	75X CR	100X CR
TP	2%	2%	2%	2%	2%	3%	2%	3%	3%
FP	23%	23%	23%	23%	23%	24%	24%	24%	24%
TN	64%	62%	61%	61%	60%	59%	59%	57%	57%
FN	11%	13%	13%	13%	14%	15%	15%	16%	17%
Accuracy	66%	64%	63%	63%	63%	61%	61%	60%	60%
FPR	27%	27%	28%	28%	28%	29%	29%	29%	29%
TR	15%	15%	15%	15%	15%	14%	14%	13%	13%

5 Sigma

	0 CR	3X CR	5X CR	10X CR	20X CR	35X CR	50X CR	75X CR	100X CR
TP	2%	2%	2%	2%	2%	2%	2%	3%	3%
FP	24%	23%	24%	24%	24%	24%	24%	24%	24%
TN	64%	61%	61%	61%	60%	58%	59%	57%	57%
FN	11%	13%	13%	13%	14%	15%	15%	17%	17%
Accuracy	66%	64%	63%	63%	62%	61%	61%	60%	59%
FPR	27%	28%	28%	28%	28%	29%	29%	29%	30%
TR	15%	15%	15%	15%	14%	14%	14%	13%	13%

10 Sigma

	0 CR	3X CR	5X CR	10X CR	20X CR	35X CR	50X CR	75X CR	100X CR
TP	2%	2%	2%	2%	2%	3%	2%	3%	3%
FP	24%	24%	25%	25%	25%	25%	25%	25%	25%
TN	63%	60%	60%	60%	59%	58%	58%	56%	56%
FN	10%	13%	13%	13%	14%	15%	15%	16%	16%
Accuracy	65%	63%	62%	62%	61%	60%	60%	59%	59%
FPR	28%	29%	29%	29%	29%	30%	30%	31%	31%
TR	15%	15%	15%	15%	15%	14%	14%	14%	14%

20 Sigma

	0 CR	3X CR	5X CR	10X CR	20X CR	35X CR	50X CR	75X CR	100X CR
TP	2%	2%	2%	2%	2%	3%	3%	3%	3%
FP	27%	27%	27%	27%	27%	27%	27%	27%	27%
TN	61%	58%	57%	57%	57%	55%	56%	54%	54%
FN	10%	13%	13%	13%	14%	15%	15%	16%	16%
Accuracy	63%	60%	60%	60%	59%	58%	58%	57%	57%
FPR	31%	32%	32%	32%	32%	33%	33%	33%	33%
TR	16%	16%	16%	16%	15%	15%	15%	14%	14%

40 Sigma

	0 CR	3X CR	5X CR	10X CR	20X CR	35X CR	50X CR	75X CR	100X CR
TP	2%	3%	3%	3%	3%	3%	3%	3%	3%
FP	31%	30%	30%	30%	30%	30%	30%	29%	29%
TN	56%	54%	54%	54%	53%	53%	53%	52%	52%
FN	10%	13%	13%	13%	14%	15%	14%	16%	16%
Accuracy	58%	57%	57%	57%	56%	55%	56%	54%	55%
FPR	36%	36%	36%	36%	36%	36%	36%	36%	36%
TR	17%	17%	17%	17%	16%	16%	16%	15%	15%

Table B-3 - Ba-133 and Ra-226 Statistical Results Based on Standard Deviation of Normal Population

1 Sigma

	Ba	0.5 Ba	Ra	0.5Ra
TP	9%	5%	2%	1%
FP	6%	3%	23%	11%
TN	81%	73%	65%	76%
FN	3%	20%	11%	12%
Accuracy	90%	77%	66%	77%
FPR	7%	3%	26%	13%
TR	73%	19%	15%	7%

2 Sigma

	Ba	0.5 Ba	Ra	0.5Ra
TP	9%	5%	2%	1%
FP	7%	3%	23%	11%
TN	81%	73%	64%	76%
FN	3%	20%	11%	12%
Accuracy	90%	77%	66%	77%
FPR	7%	4%	26%	13%
TR	73%	19%	15%	7%

3 Sigma

	Ba	0.5 Ba	Ra	0.5Ra
TP	9%	5%	2%	1%
FP	7%	3%	23%	11%
TN	81%	72%	64%	76%
FN	3%	20%	11%	12%
Accuracy	90%	77%	66%	77%
FPR	8%	4%	27%	13%
TR	73%	19%	15%	7%

5 Sigma

	Ba	0.5 Ba	Ra	0.5Ra
TP	9%	5%	2%	1%
FP	7%	3%	24%	11%
TN	81%	72%	64%	76%
FN	3%	20%	11%	12%
Accuracy	90%	77%	66%	77%
FPR	8%	4%	27%	13%
TR	73%	19%	15%	7%

10 Sigma

	Ba	0.5 Ba	Ra	0.5Ra
TP	9%	5%	2%	1%
FP	6%	2%	24%	11%
TN	81%	73%	63%	76%
FN	3%	20%	10%	12%
Accuracy	90%	77%	65%	77%
FPR	7%	3%	28%	13%
TR	72%	19%	15%	7%

20 Sigma

	Ba	0.5 Ba	Ra	0.5Ra
TP	9%	5%	2%	1%
FP	6%	2%	27%	12%
TN	82%	73%	61%	75%
FN	3%	20%	10%	12%
Accuracy	91%	78%	63%	76%
FPR	7%	3%	31%	14%
TR	72%	19%	16%	7%

40 Sigma

	Ba	0.5 Ba	Ra	0.5Ra
TP	9%	5%	2%	1%
FP	6%	2%	31%	16%
TN	82%	73%	56%	72%
FN	4%	20%	10%	12%
Accuracy	91%	78%	58%	73%
FPR	7%	3%	36%	18%
TR	71%	19%	17%	6%

APPENDIX C. PARALLEL INVESTIGATIONS

Although not explicitly called out in the statement of work, the following figures illustrate the ideal discrimination capability of the algorithm when comparing a desired source (WGPu or HEU) to various undesired sources. These results illustrate the increase in performance with higher spectral resolution (HPGe vs. NaI detectors)

C.1. IdentiFINDER vs. ORTEC Detective

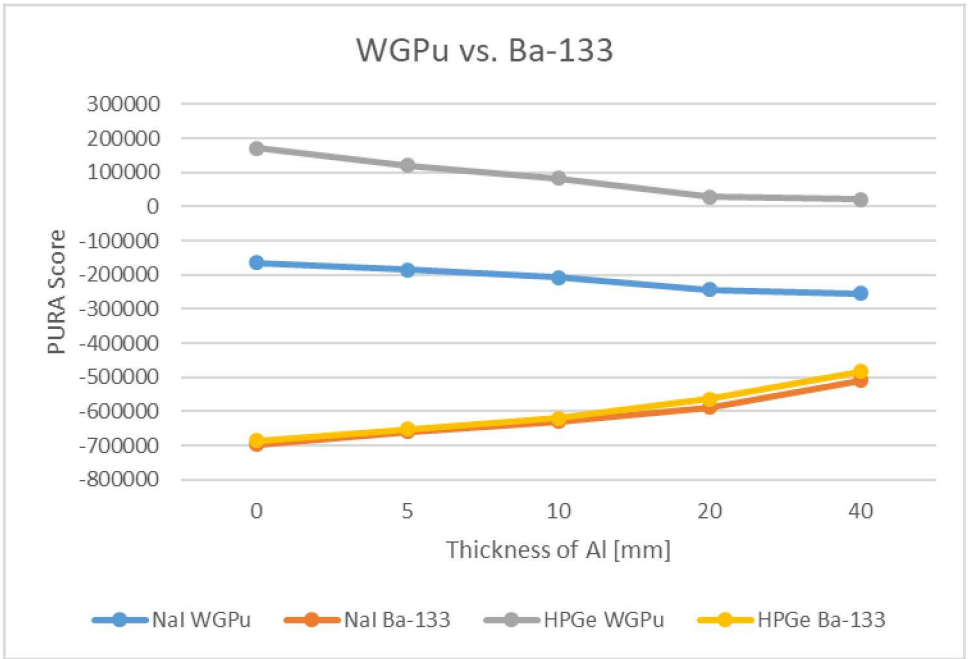

Figure 19 - WGPu vs. Ba-133 Discrimination

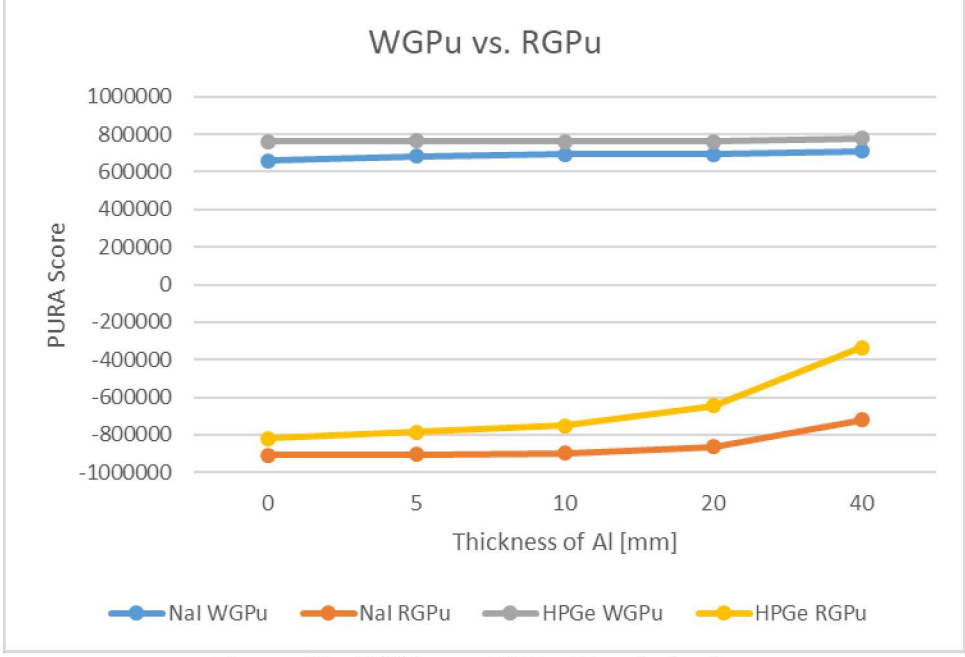

Figure 20 - WGPu vs. RGPu Discrimination

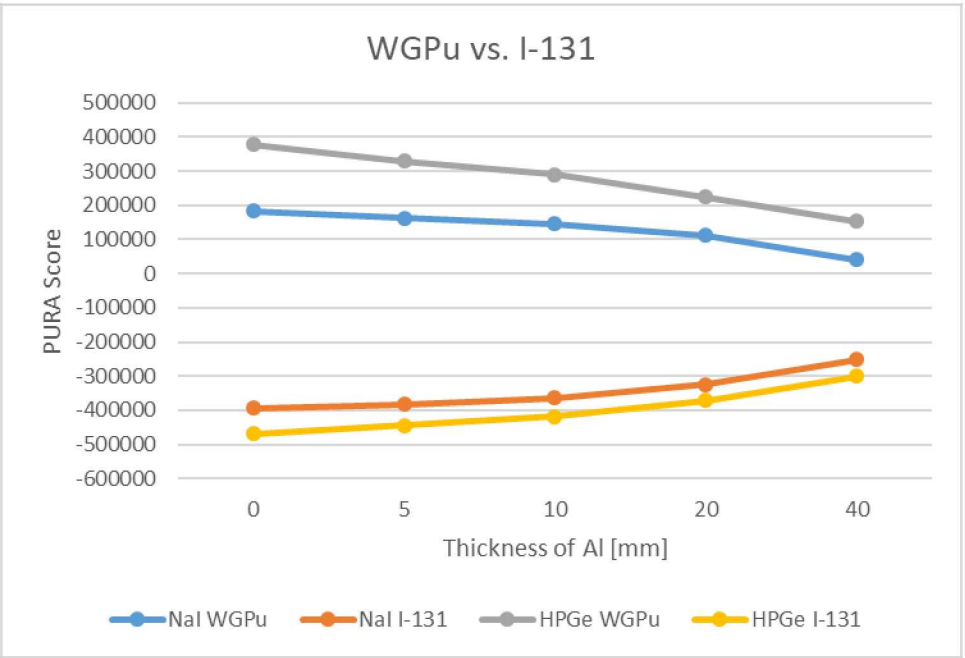

Figure 21 - WGPu vs. I-131 Discrimination

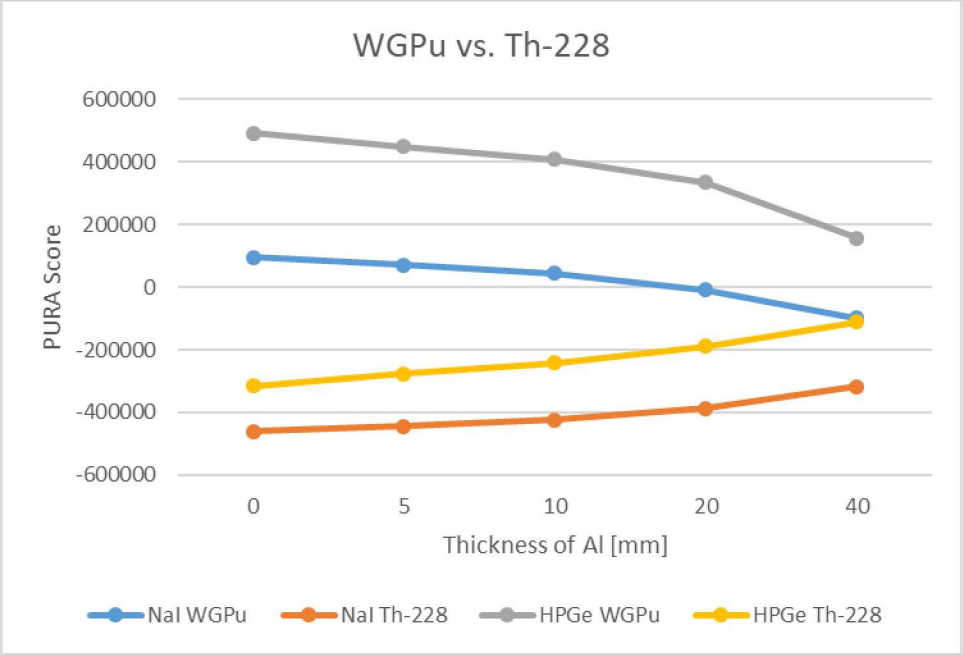

Figure 22 - WGPu vs. Th-228 Discrimination

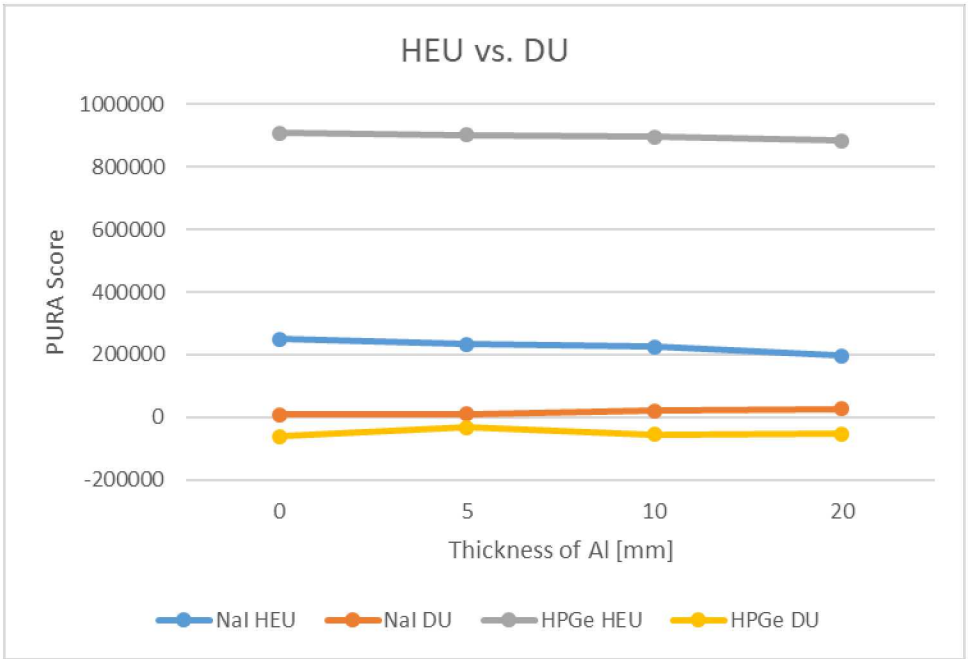

Figure 23 - HEU vs. DU Discrimination

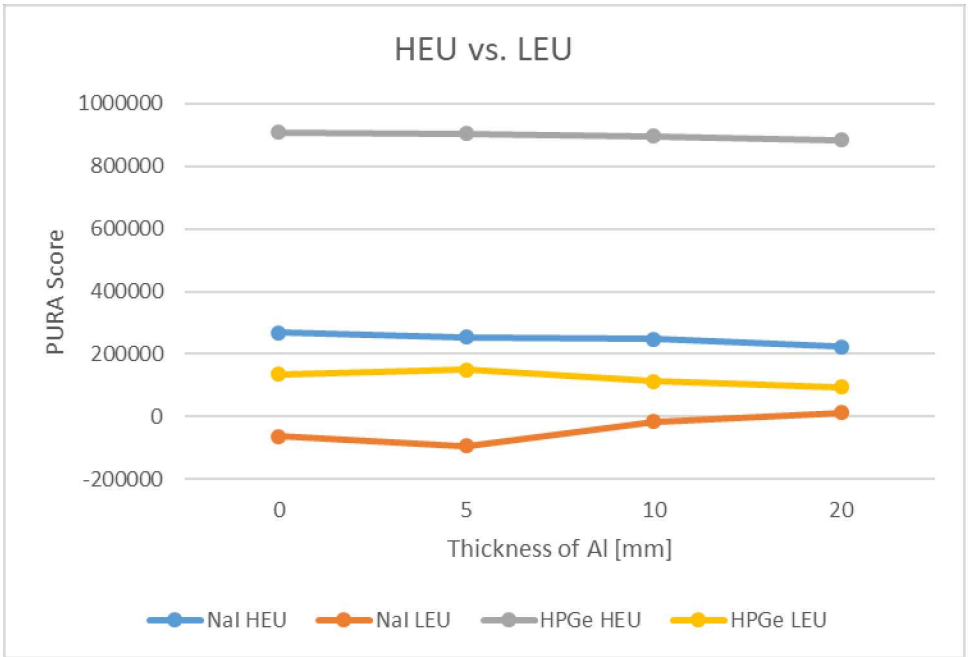

Figure 24 - HEU vs. LEU Discrimination

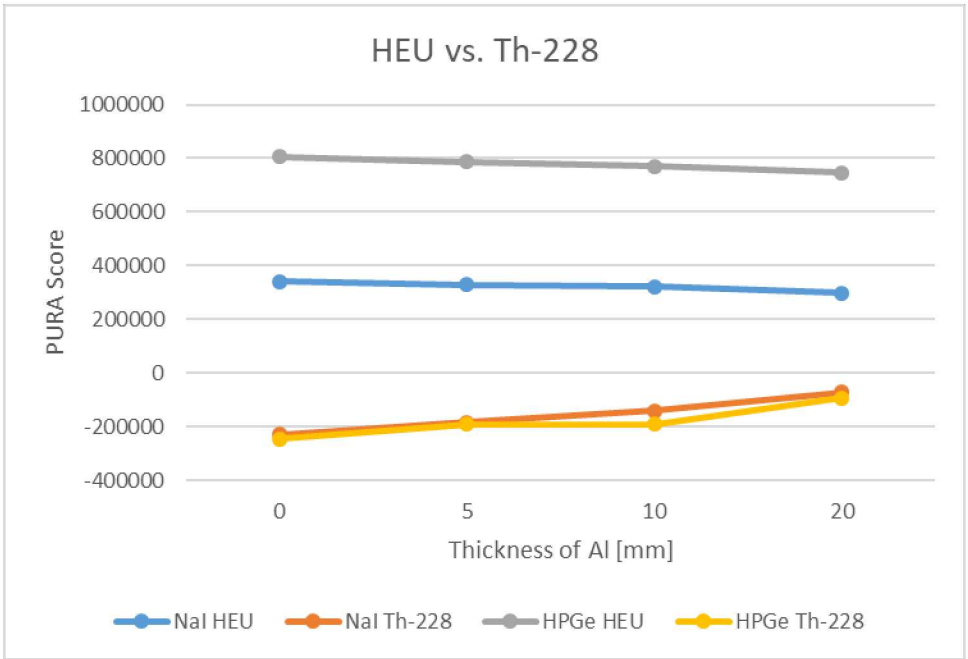

Figure 25 - HEU vs. Th-228 Discrimination

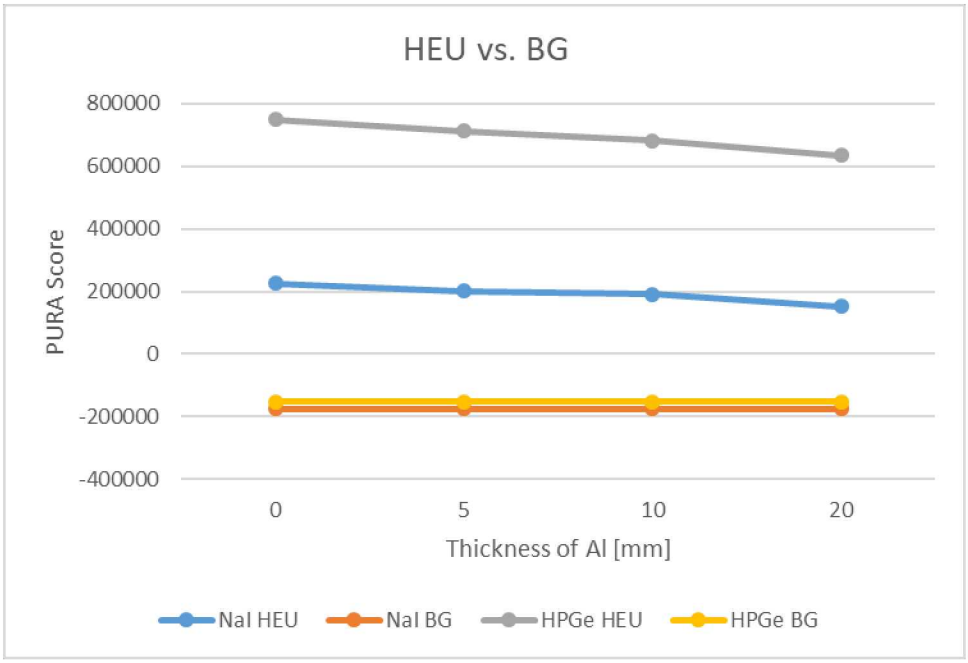

Figure 26 - HEU vs. BG Discrimination

C.2. Performance vs. Resolution and Weight Array Thresholds

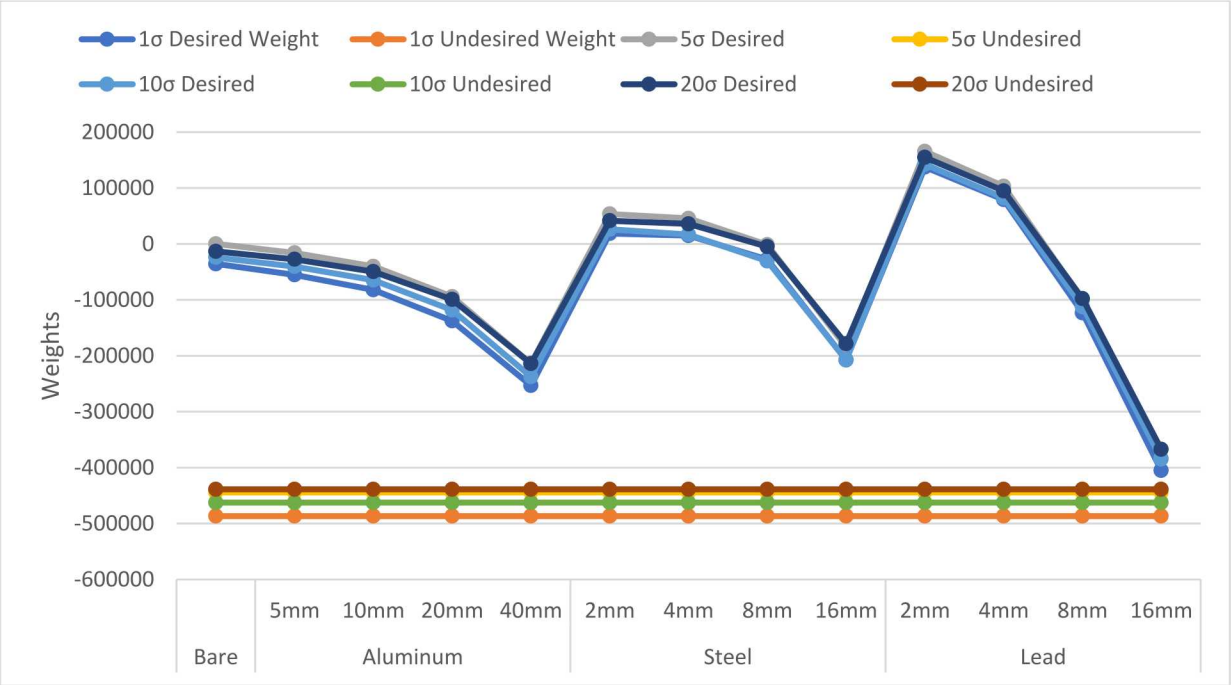

Figure 27 - WGPu vs. Background with 1% Resolution

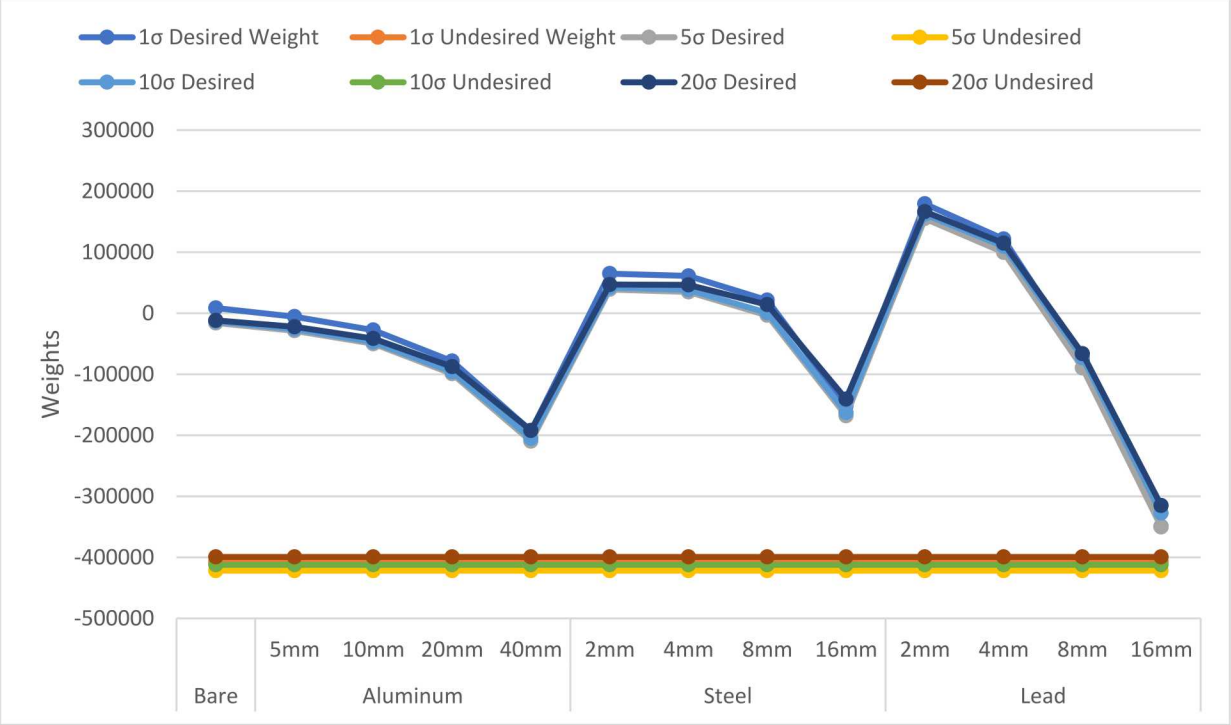

Figure 28 - WGPu vs. Background with 6.4% Resolution

Figure 29 - WGPu vs. Background with 10% Resolution

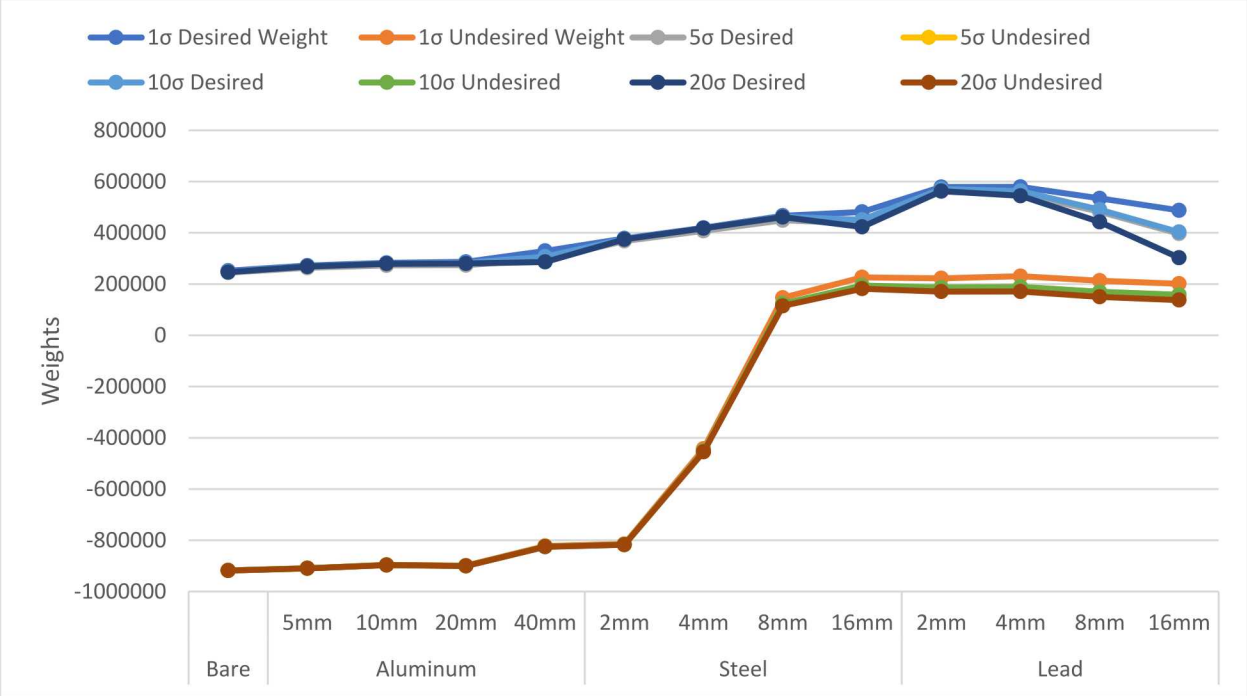

Figure 30 - WGPu vs. RGPu with 1% Resolution

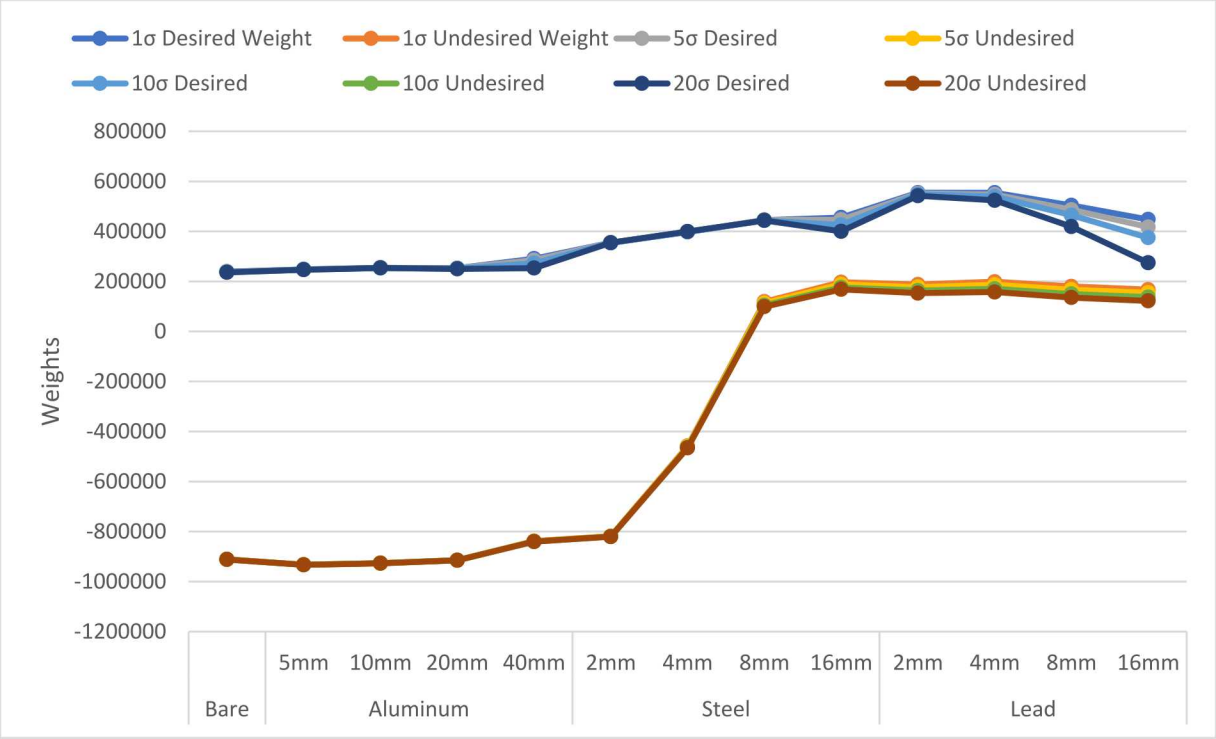

Figure 31 - WGPu vs. RGPu with 6.4% Resolution

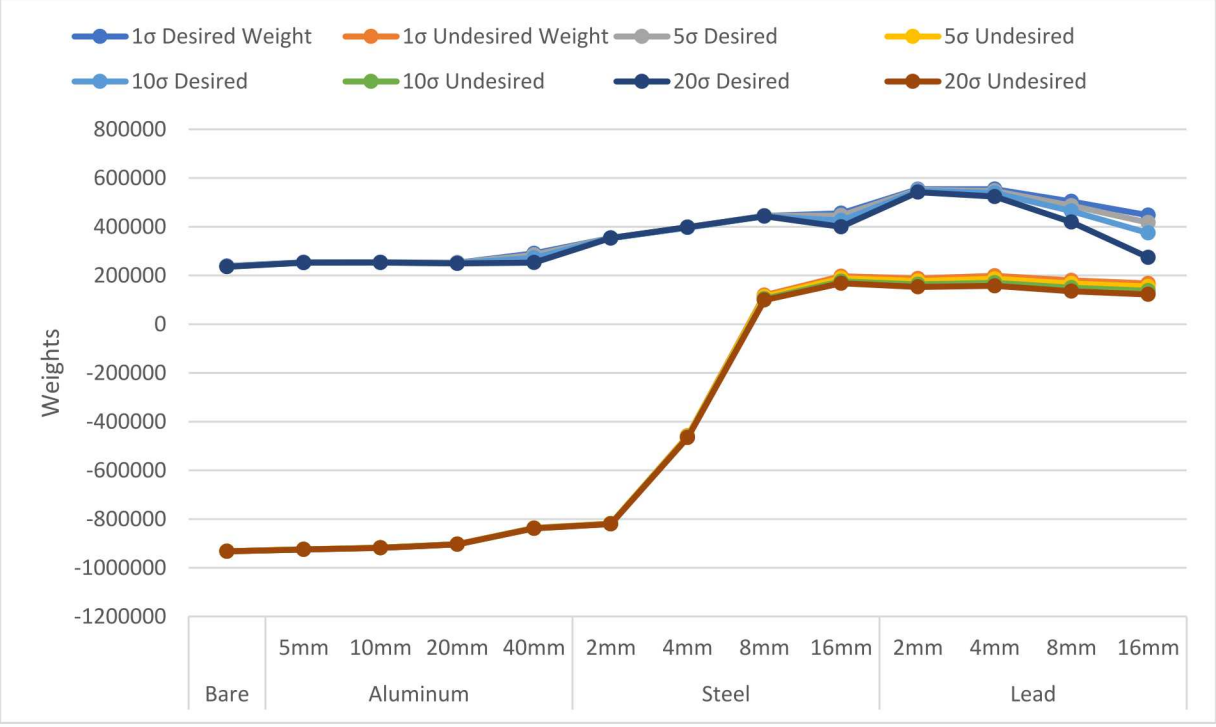

Figure 32 - WGPu vs. RGPu with 10% Resolution

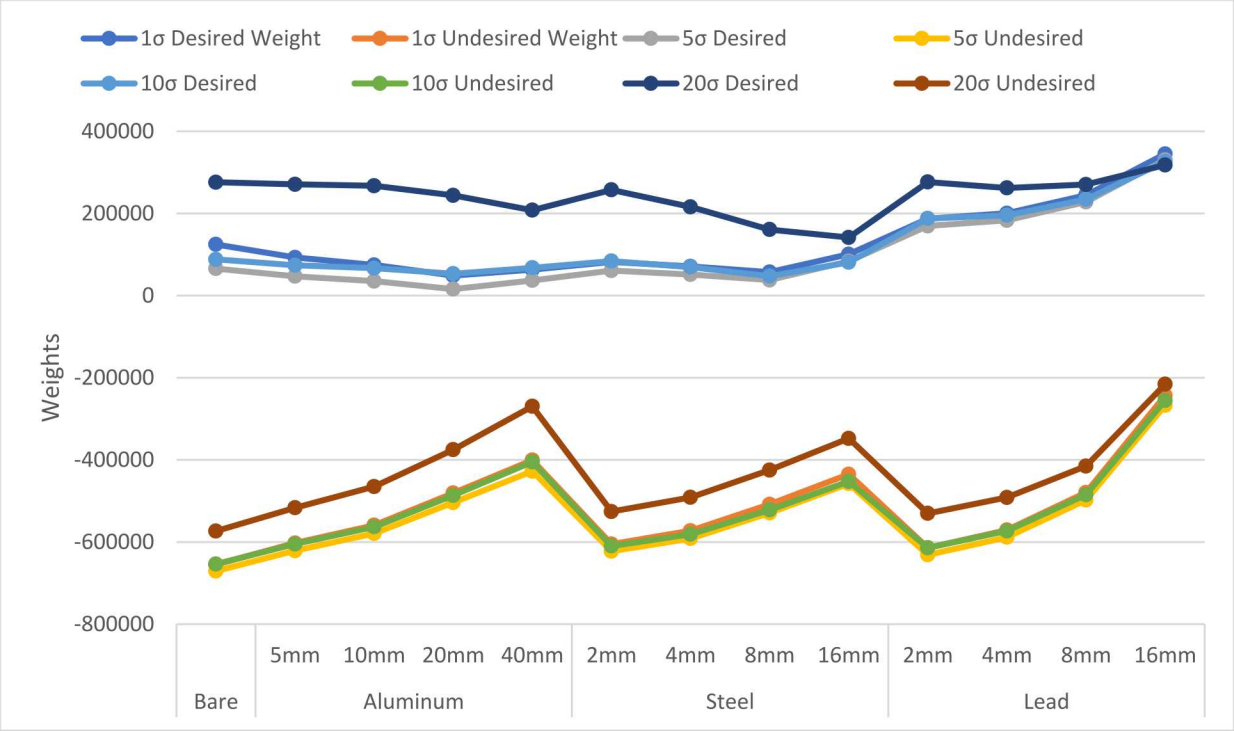

Figure 33 - WGPu vs. I-131 with 1% Resolution

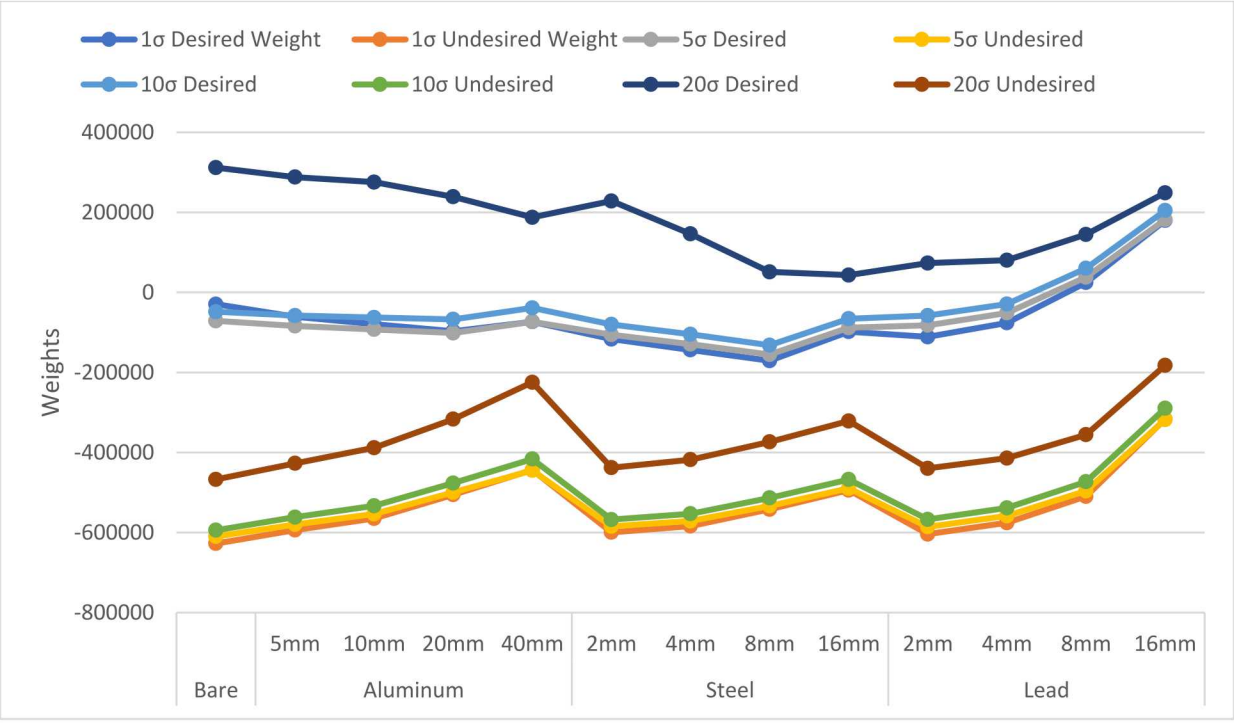

Figure 34 - WGPu vs. I-131 with 6.4% Resolution

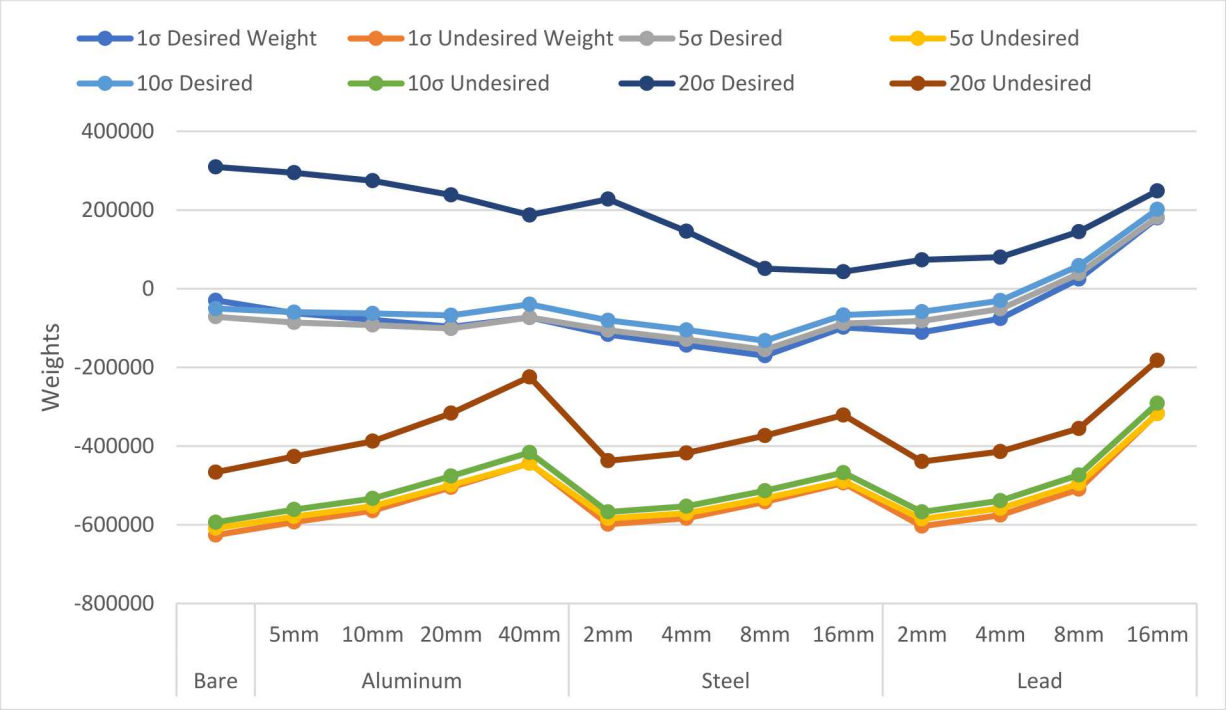

Figure 35 - WGPu vs. I-131 with 10% Resolution

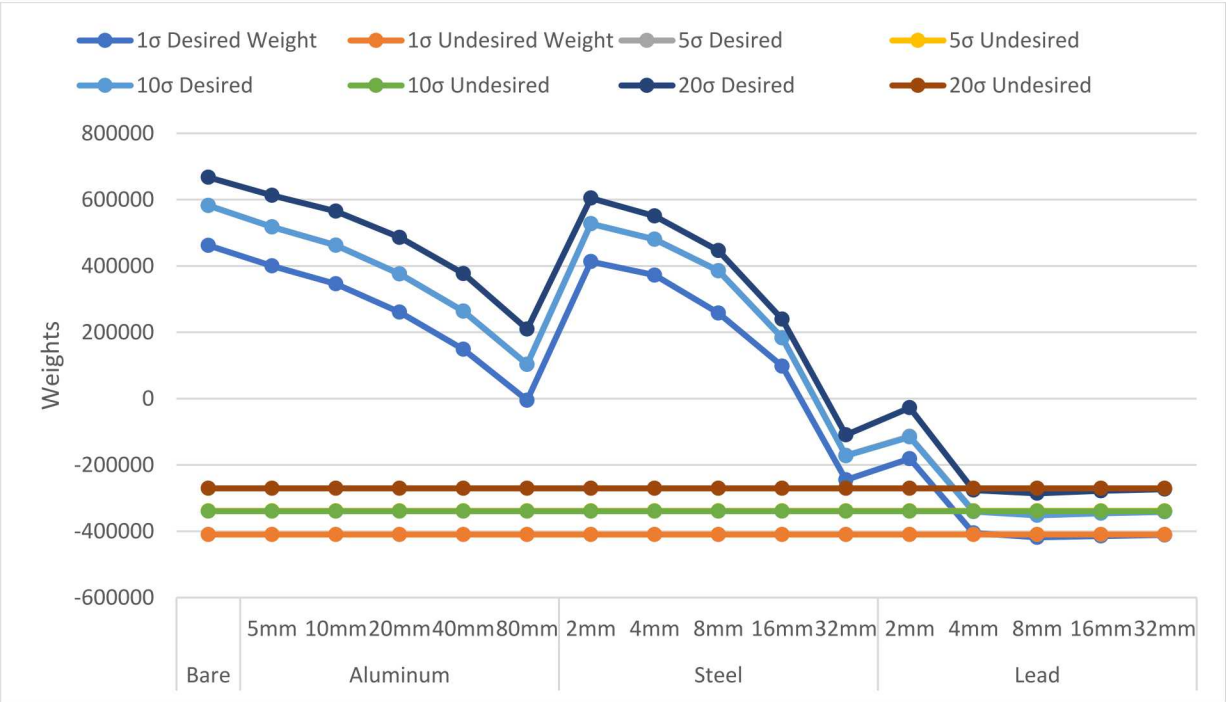

Figure 36 - HEU vs. Background with 1% Resolution

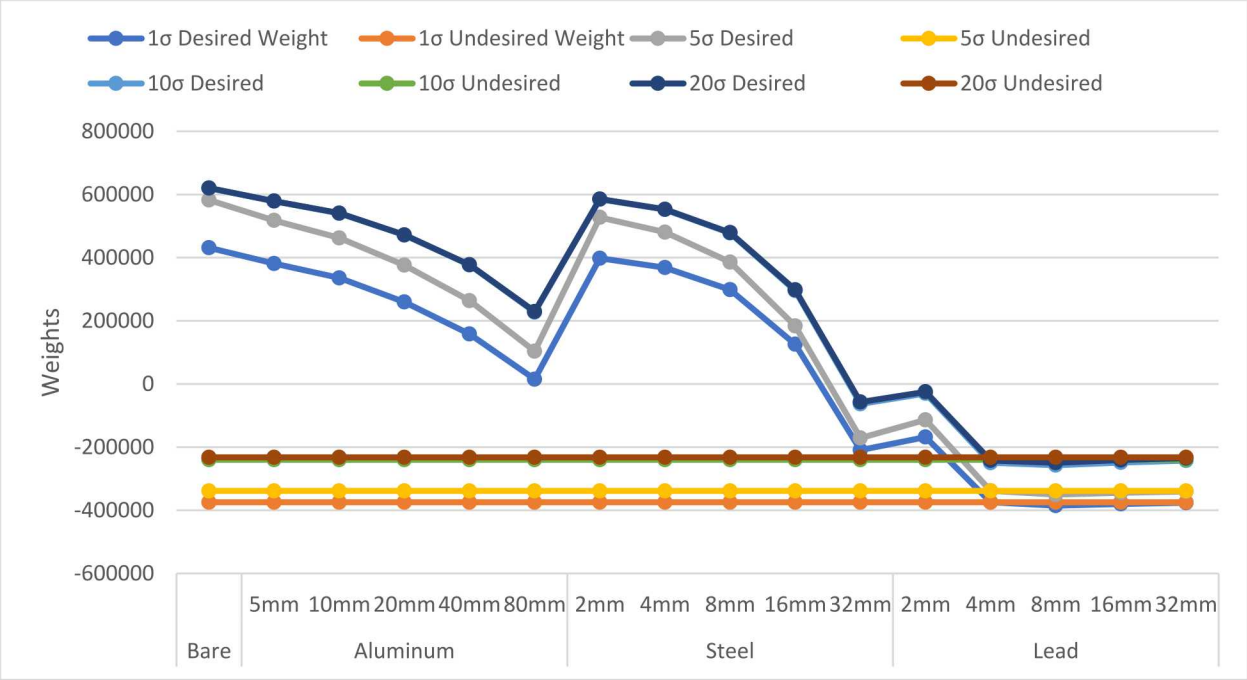

Figure 37 - HEU vs. Background with 6.4% Resolution

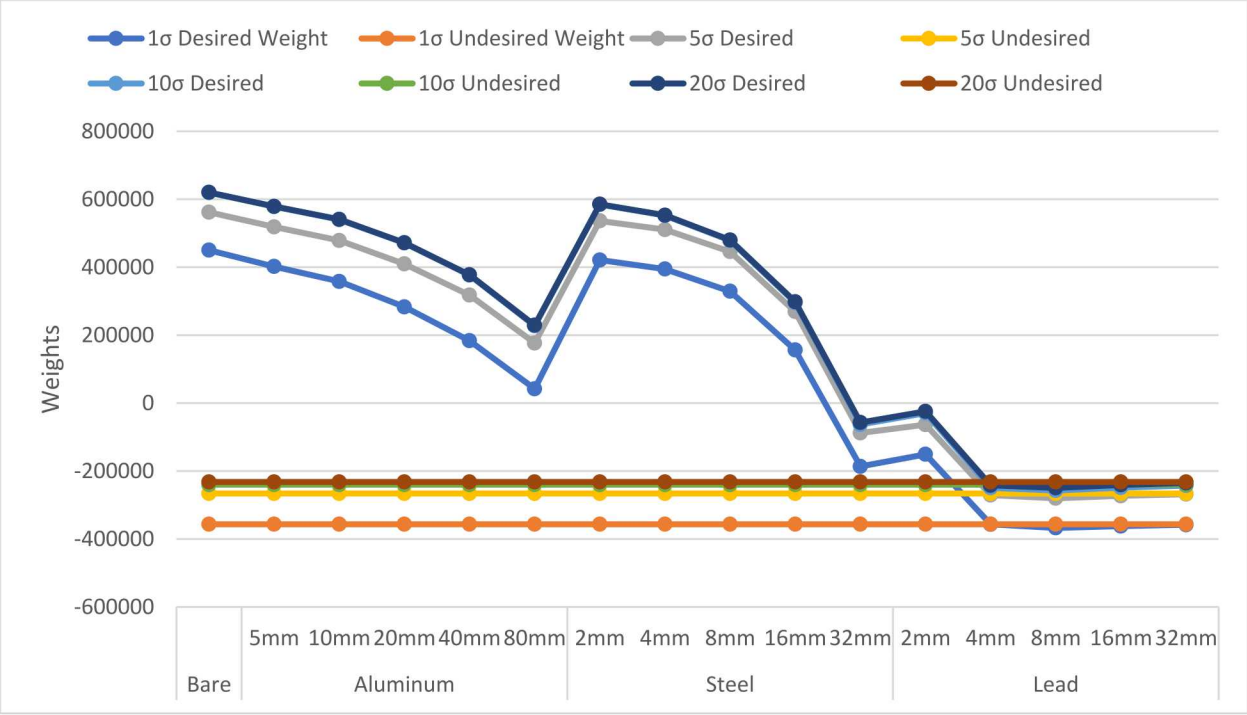

Figure 38 - HEU vs. Background with 10% Resolution

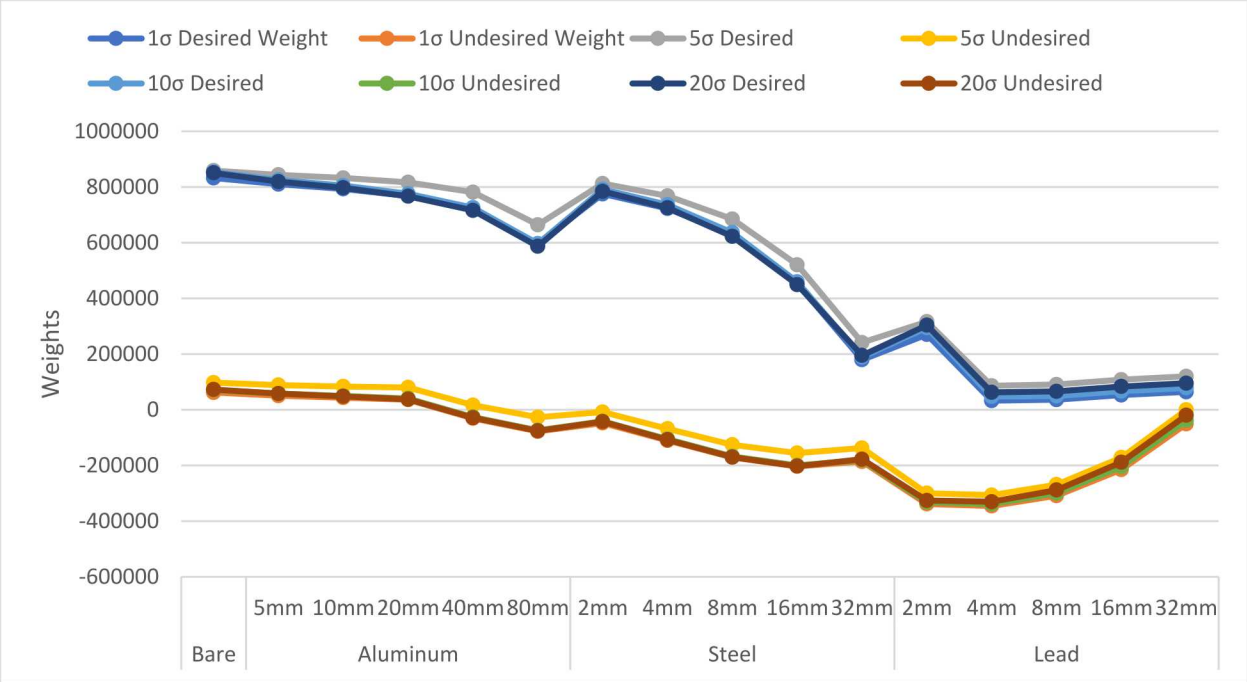

Figure 39 - HEU vs. LEU with 1% Resolution

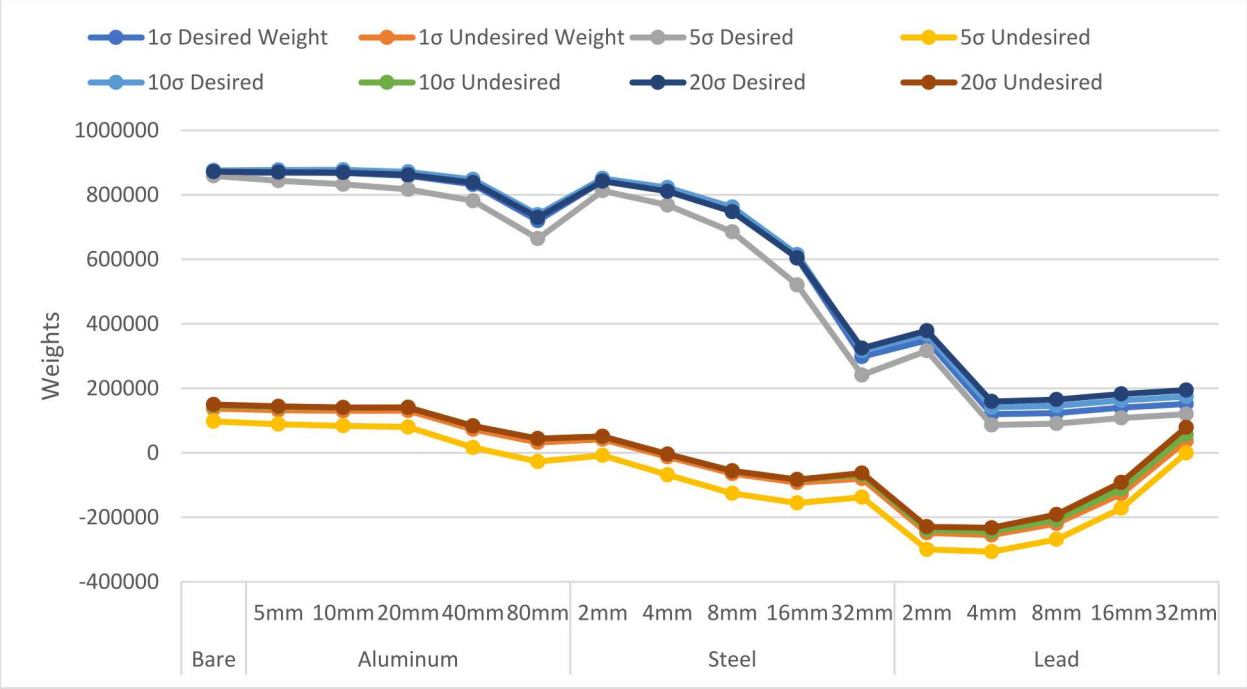

Figure 40 - HEU vs. LEU with 6.4% Resolution

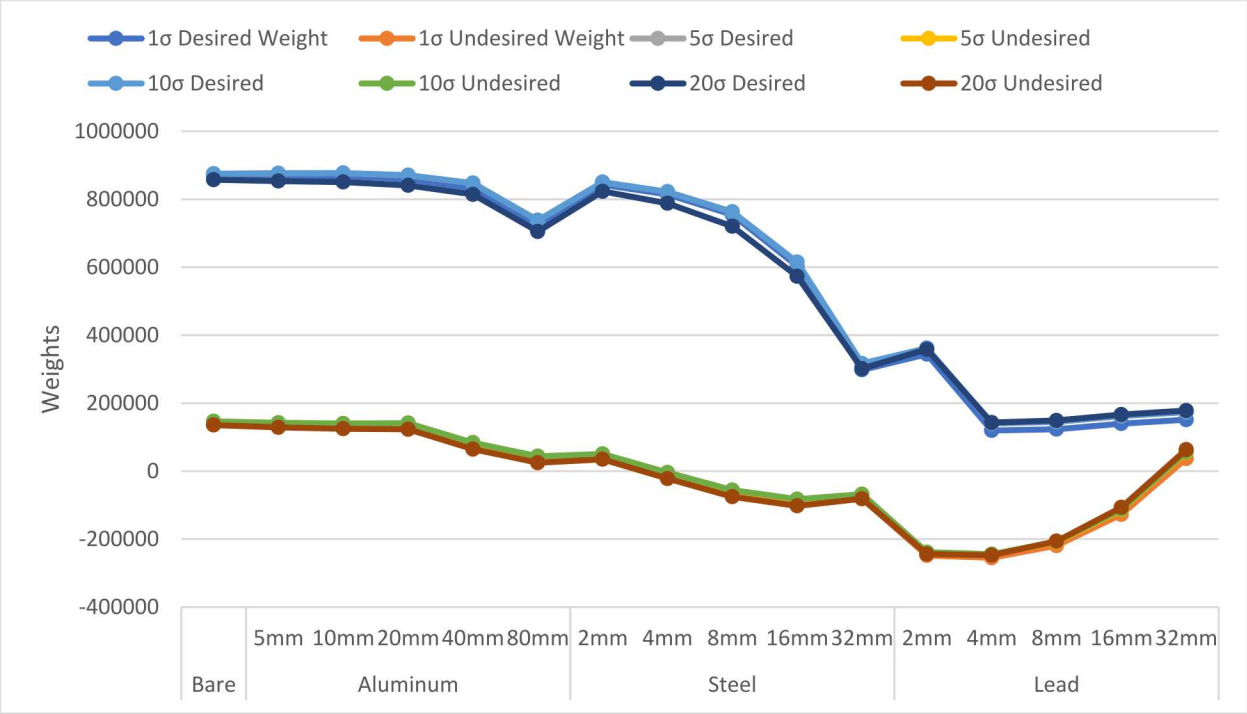

Figure 41 - HEU vs. LEU with 10% Resolution

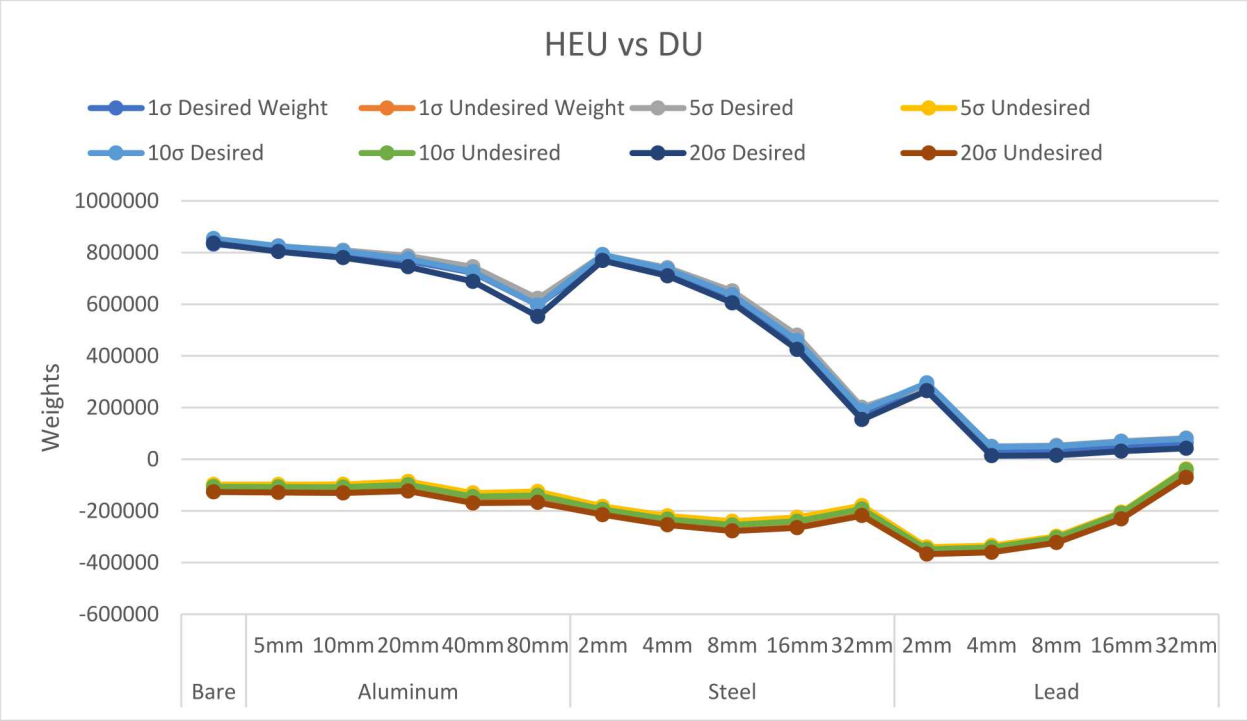

Figure 42 - HEU vs. DU with 1% Resolution

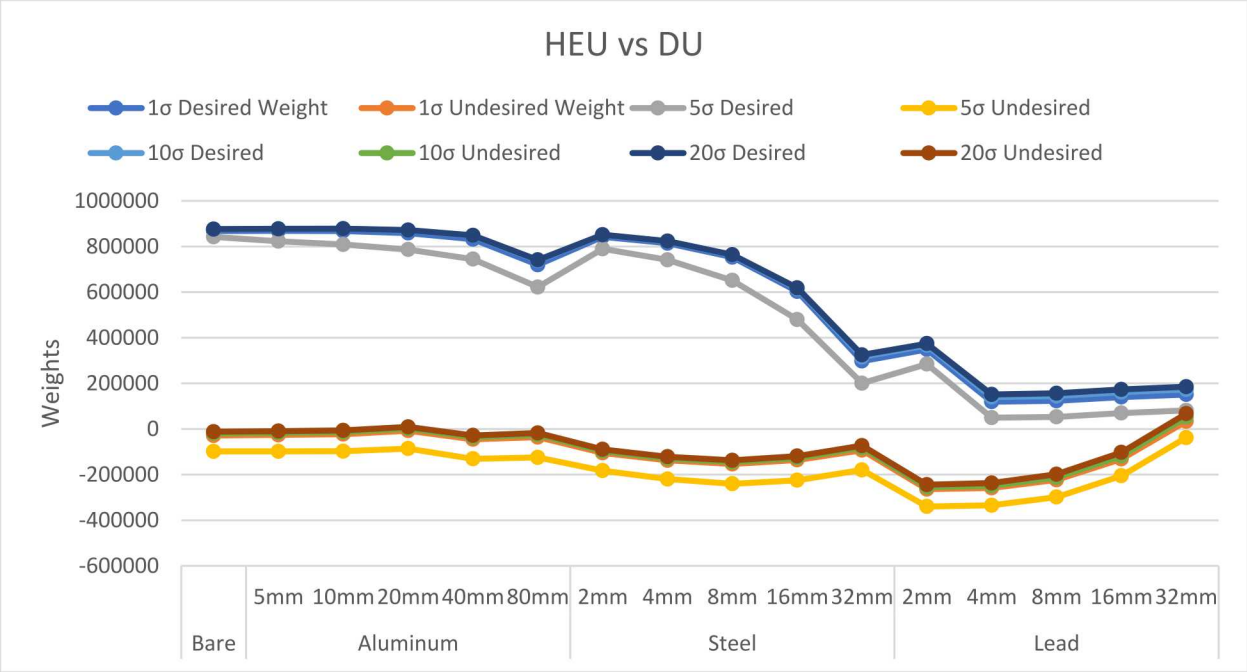

Figure 43 - HEU vs. DU with 6.4% Resolution

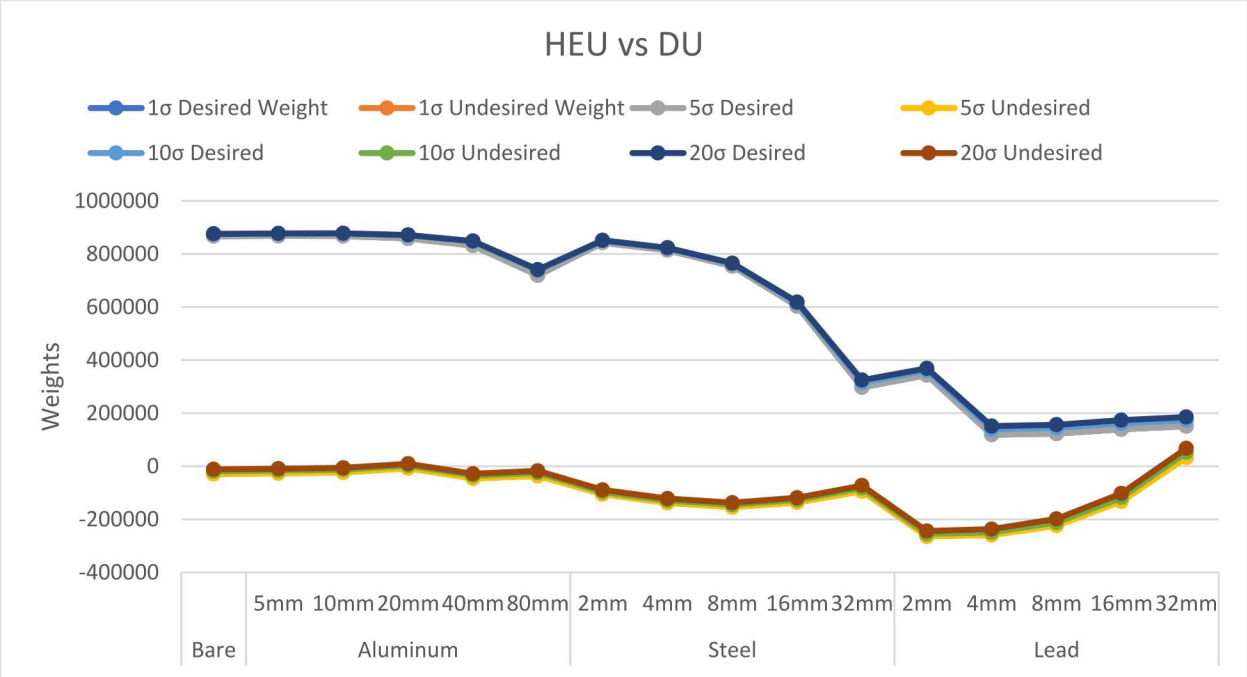

Figure 44 - HEU vs. DU with 10% Resolution

APPENDIX D. LIST OF SOURCES AND SHIELDING

The following table lists all simulated spectra which were generated to test the algorithm. For all Ba-133 and Ra-226 spectra, an individually optimized weight array was generated for each of those desired spectrum versus each undesired spectrum, resulting in a total of 214,130 desired vs. undesired weight arrays (comparisons).

Table D-4. Simulated Source Shielding Configurations

Isotope	Shielding Material	Shielding Thickness (In)	Strength (μCi)
Ba133	Al	0.25	1000
Ba133	Al	0.5	1000
Ba133	Al	0.75	1000
Ba133	Al	1	1000
Ba133	Al	1.5	1000
Ba133	Al	3	1000
Ba133	Bare	0	1000
Ba133	Pb	0.03125	1000
Ba133	Pb	0.0625	1000
Ba133	Pb	0.125	1000
Ba133	Pb	0.25	1000
Ba133	Pb	0.5	1000
Ba133	Pb	1000	1000
Ba133	Steel	0.125	1000
Ba133	Steel	0.25	1000
Ba133	Steel	0.5	1000
Ba133	Steel	0.75	1000
Ba133	Steel	10	1000
Ba133	Steel	1.5	1000
Ba133	Al	0.25	100
Ba133	Al	0.5	100
Ba133	Al	0.75	100
Ba133	Al	1	100
Ba133	Al	1.5	100
Ba133	Al	3	100
Ba133	Bare	0	100
Ba133	Pb	0.03125	100
Ba133	Pb	0.0625	100
Ba133	Pb	0.125	100
Ba133	Pb	0.25	100
Ba133	Pb	0.5	100
Ba133	Pb	1000	100
Ba133	Steel	0.125	100
Ba133	Steel	0.25	100

Isotope	Shielding Material	Shielding Thickness (In)	Strength (μCi)
Ba133	Steel	0.5	100
Ba133	Steel	0.75	100
Ba133	Steel	10	100
Ba133	Steel	1.5	100
Ba133	Al	0.25	10
Ba133	Al	0.5	10
Ba133	Al	0.75	10
Ba133	Al	1	10
Ba133	Al	1.5	10
Ba133	Al	3	10
Ba133	Bare	0	10
Ba133	Pb	0.03125	10
Ba133	Pb	0.0625	10
Ba133	Pb	0.125	10
Ba133	Pb	0.25	10
Ba133	Pb	0.5	10
Ba133	Pb	1000	10
Ba133	Steel	0.125	10
Ba133	Steel	0.25	10
Ba133	Steel	0.5	10
Ba133	Steel	0.75	10
Ba133	Steel	10	10
Ba133	Steel	1.5	10
Ba133	Al	0.25	200
Ba133	Al	0.5	200
Ba133	Al	0.75	200
Ba133	Al	1	200
Ba133	Al	1.5	200
Ba133	Al	3	200
Ba133	Bare	0	200
Ba133	Pb	0.03125	200
Ba133	Pb	0.0625	200
Ba133	Pb	0.125	200
Ba133	Pb	0.25	200
Ba133	Pb	0.5	200
Ba133	Pb	1000	200
Ba133	Steel	0.125	200
Ba133	Steel	0.25	200
Ba133	Steel	0.5	200
Ba133	Steel	0.75	200

Isotope	Shielding Material	Shielding Thickness (In)	Strength (μCi)
Ba133	Steel	10	200
Ba133	Steel	1.5	200
Ba133	Al	0.25	350
Ba133	Al	0.5	350
Ba133	Al	0.75	350
Ba133	Al	1	350
Ba133	Al	1.5	350
Ba133	Al	3	350
Ba133	Bare	0	350
Ba133	Pb	0.03125	350
Ba133	Pb	0.0625	350
Ba133	Pb	0.125	350
Ba133	Pb	0.25	350
Ba133	Pb	0.5	350
Ba133	Pb	1000	350
Ba133	Steel	0.125	350
Ba133	Steel	0.25	350
Ba133	Steel	0.5	350
Ba133	Steel	0.75	350
Ba133	Steel	10	350
Ba133	Steel	1.5	350
Ba133	Al	0.25	500
Ba133	Al	0.5	500
Ba133	Al	0.75	500
Ba133	Al	1	500
Ba133	Al	1.5	500
Ba133	Al	3	500
Ba133	Bare	0	500
Ba133	Pb	0.03125	500
Ba133	Pb	0.0625	500
Ba133	Pb	0.125	500
Ba133	Pb	0.25	500
Ba133	Pb	0.5	500
Ba133	Pb	1000	500
Ba133	Steel	0.125	500
Ba133	Steel	0.25	500
Ba133	Steel	0.5	500
Ba133	Steel	0.75	500
Ba133	Steel	10	500
Ba133	Steel	1.5	500

Isotope	Shielding Material	Shielding Thickness (In)	Strength (μCi)
Ba133	Al	0.25	750
Ba133	Al	0.5	750
Ba133	Al	0.75	750
Ba133	Al	1	750
Ba133	Al	1.5	750
Ba133	Al	3	750
Ba133	Bare	0	750
Ba133	Pb	0.03125	750
Ba133	Pb	0.0625	750
Ba133	Pb	0.125	750
Ba133	Pb	0.25	750
Ba133	Pb	0.5	750
Ba133	Pb	1000	750
Ba133	Steel	0.125	750
Ba133	Steel	0.25	750
Ba133	Steel	0.5	750
Ba133	Steel	0.75	750
Ba133	Steel	10	750
Ba133	Steel	1.5	750
Background	0	0	1000
Background	0	0	100
Background	0	0	10
Background	0	0	200
Background	0	0	350
Background	0	0	500
Background	0	0	750
Cd109	Al	0.25	1000
Cd109	Al	0.5	1000
Cd109	Al	0.75	1000
Cd109	Al	1	1000
Cd109	Al	1.5	1000
Cd109	Al	3	1000
Cd109	Bare	0	1000
Cd109	Pb	0.03125	1000
Cd109	Pb	0.0625	1000
Cd109	Pb	0.125	1000
Cd109	Pb	0.25	1000
Cd109	Pb	0.5	1000
Cd109	Pb	1000	1000
Cd109	Steel	0.125	1000

Isotope	Shielding Material	Shielding Thickness (In)	Strength (μCi)
Cd109	Steel	0.25	1000
Cd109	Steel	0.5	1000
Cd109	Steel	0.75	1000
Cd109	Steel	10	1000
Cd109	Steel	1.5	1000
Cd109	Al	0.25	100
Cd109	Al	0.5	100
Cd109	Al	0.75	100
Cd109	Al	1	100
Cd109	Al	1.5	100
Cd109	Al	3	100
Cd109	Bare	0	100
Cd109	Pb	0.03125	100
Cd109	Pb	0.0625	100
Cd109	Pb	0.125	100
Cd109	Pb	0.25	100
Cd109	Pb	0.5	100
Cd109	Pb	1000	100
Cd109	Steel	0.125	100
Cd109	Steel	0.25	100
Cd109	Steel	0.5	100
Cd109	Steel	0.75	100
Cd109	Steel	10	100
Cd109	Steel	1.5	100
Cd109	Al	0.25	10
Cd109	Al	0.5	10
Cd109	Al	0.75	10
Cd109	Al	1	10
Cd109	Al	1.5	10
Cd109	Al	3	10
Cd109	Bare	0	10
Cd109	Pb	0.03125	10
Cd109	Pb	0.0625	10
Cd109	Pb	0.125	10
Cd109	Pb	0.25	10
Cd109	Pb	0.5	10
Cd109	Pb	1000	10
Cd109	Steel	0.125	10
Cd109	Steel	0.25	10
Cd109	Steel	0.5	10

Isotope	Shielding Material	Shielding Thickness (In)	Strength (μCi)
Cd109	Steel	0.75	10
Cd109	Steel	10	10
Cd109	Steel	1.5	10
Cd109	Al	0.25	200
Cd109	Al	0.5	200
Cd109	Al	0.75	200
Cd109	Al	1	200
Cd109	Al	1.5	200
Cd109	Al	3	200
Cd109	Bare	0	200
Cd109	Pb	0.03125	200
Cd109	Pb	0.0625	200
Cd109	Pb	0.125	200
Cd109	Pb	0.25	200
Cd109	Pb	0.5	200
Cd109	Pb	1000	200
Cd109	Steel	0.125	200
Cd109	Steel	0.25	200
Cd109	Steel	0.5	200
Cd109	Steel	0.75	200
Cd109	Steel	10	200
Cd109	Steel	1.5	200
Cd109	Al	0.25	350
Cd109	Al	0.5	350
Cd109	Al	0.75	350
Cd109	Al	1	350
Cd109	Al	1.5	350
Cd109	Al	3	350
Cd109	Bare	0	350
Cd109	Pb	0.03125	350
Cd109	Pb	0.0625	350
Cd109	Pb	0.125	350
Cd109	Pb	0.25	350
Cd109	Pb	0.5	350
Cd109	Pb	1000	350
Cd109	Steel	0.125	350
Cd109	Steel	0.25	350
Cd109	Steel	0.5	350
Cd109	Steel	0.75	350
Cd109	Steel	10	350

Isotope	Shielding Material	Shielding Thickness (In)	Strength (μCi)
Cd109	Steel	1.5	350
Cd109	Al	0.25	500
Cd109	Al	0.5	500
Cd109	Al	0.75	500
Cd109	Al	1	500
Cd109	Al	1.5	500
Cd109	Al	3	500
Cd109	Bare	0	500
Cd109	Pb	0.03125	500
Cd109	Pb	0.0625	500
Cd109	Pb	0.125	500
Cd109	Pb	0.25	500
Cd109	Pb	0.5	500
Cd109	Pb	1000	500
Cd109	Steel	0.125	500
Cd109	Steel	0.25	500
Cd109	Steel	0.5	500
Cd109	Steel	0.75	500
Cd109	Steel	10	500
Cd109	Steel	1.5	500
Cd109	Al	0.25	750
Cd109	Al	0.5	750
Cd109	Al	0.75	750
Cd109	Al	1	750
Cd109	Al	1.5	750
Cd109	Al	3	750
Cd109	Bare	0	750
Cd109	Pb	0.03125	750
Cd109	Pb	0.0625	750
Cd109	Pb	0.125	750
Cd109	Pb	0.25	750
Cd109	Pb	0.5	750
Cd109	Pb	1000	750
Cd109	Steel	0.125	750
Cd109	Steel	0.25	750
Cd109	Steel	0.5	750
Cd109	Steel	0.75	750
Cd109	Steel	10	750
Cd109	Steel	1.5	750
Co57	Al	0.25	1000

Isotope	Shielding Material	Shielding Thickness (In)	Strength (μCi)
Co57	Al	0.5	1000
Co57	Al	0.75	1000
Co57	Al	1	1000
Co57	Al	1.5	1000
Co57	Al	3	1000
Co57	Bare	0	1000
Co57	Pb	0.03125	1000
Co57	Pb	0.0625	1000
Co57	Pb	0.125	1000
Co57	Pb	0.25	1000
Co57	Pb	0.5	1000
Co57	Pb	1000	1000
Co57	Steel	0.125	1000
Co57	Steel	0.25	1000
Co57	Steel	0.5	1000
Co57	Steel	0.75	1000
Co57	Steel	10	1000
Co57	Steel	1.5	1000
Co57	Al	0.25	100
Co57	Al	0.5	100
Co57	Al	0.75	100
Co57	Al	1	100
Co57	Al	1.5	100
Co57	Al	3	100
Co57	Bare	0	100
Co57	Pb	0.03125	100
Co57	Pb	0.0625	100
Co57	Pb	0.125	100
Co57	Pb	0.25	100
Co57	Pb	0.5	100
Co57	Pb	1000	100
Co57	Steel	0.125	100
Co57	Steel	0.25	100
Co57	Steel	0.5	100
Co57	Steel	0.75	100
Co57	Steel	10	100
Co57	Steel	1.5	100
Co57	Al	0.25	10
Co57	Al	0.5	10
Co57	Al	0.75	10

Isotope	Shielding Material	Shielding Thickness (In)	Strength (μCi)
Co57	Al	1	10
Co57	Al	1.5	10
Co57	Al	3	10
Co57	Bare	0	10
Co57	Pb	0.03125	10
Co57	Pb	0.0625	10
Co57	Pb	0.125	10
Co57	Pb	0.25	10
Co57	Pb	0.5	10
Co57	Pb	1000	10
Co57	Steel	0.125	10
Co57	Steel	0.25	10
Co57	Steel	0.5	10
Co57	Steel	0.75	10
Co57	Steel	10	10
Co57	Steel	1.5	10
Co57	Al	0.25	200
Co57	Al	0.5	200
Co57	Al	0.75	200
Co57	Al	1	200
Co57	Al	1.5	200
Co57	Al	3	200
Co57	Bare	0	200
Co57	Pb	0.03125	200
Co57	Pb	0.0625	200
Co57	Pb	0.125	200
Co57	Pb	0.25	200
Co57	Pb	0.5	200
Co57	Pb	1000	200
Co57	Steel	0.125	200
Co57	Steel	0.25	200
Co57	Steel	0.5	200
Co57	Steel	0.75	200
Co57	Steel	10	200
Co57	Steel	1.5	200
Co57	Al	0.25	350
Co57	Al	0.5	350
Co57	Al	0.75	350
Co57	Al	1	350
Co57	Al	1.5	350

Isotope	Shielding Material	Shielding Thickness (In)	Strength (μCi)
Co57	Al	3	350
Co57	Bare	0	350
Co57	Pb	0.03125	350
Co57	Pb	0.0625	350
Co57	Pb	0.125	350
Co57	Pb	0.25	350
Co57	Pb	0.5	350
Co57	Pb	1000	350
Co57	Steel	0.125	350
Co57	Steel	0.25	350
Co57	Steel	0.5	350
Co57	Steel	0.75	350
Co57	Steel	10	350
Co57	Steel	1.5	350
Co57	Al	0.25	500
Co57	Al	0.5	500
Co57	Al	0.75	500
Co57	Al	1	500
Co57	Al	1.5	500
Co57	Al	3	500
Co57	Bare	0	500
Co57	Pb	0.03125	500
Co57	Pb	0.0625	500
Co57	Pb	0.125	500
Co57	Pb	0.25	500
Co57	Pb	0.5	500
Co57	Pb	1000	500
Co57	Steel	0.125	500
Co57	Steel	0.25	500
Co57	Steel	0.5	500
Co57	Steel	0.75	500
Co57	Steel	10	500
Co57	Steel	1.5	500
Co57	Al	0.25	750
Co57	Al	0.5	750
Co57	Al	0.75	750
Co57	Al	1	750
Co57	Al	1.5	750
Co57	Al	3	750
Co57	Bare	0	750

Isotope	Shielding Material	Shielding Thickness (In)	Strength (μCi)
Co57	Pb	0.03125	750
Co57	Pb	0.0625	750
Co57	Pb	0.125	750
Co57	Pb	0.25	750
Co57	Pb	0.5	750
Co57	Pb	1000	750
Co57	Steel	0.125	750
Co57	Steel	0.25	750
Co57	Steel	0.5	750
Co57	Steel	0.75	750
Co57	Steel	10	750
Co57	Steel	1.5	750
Co60	Al	0.25	1000
Co60	Al	0.5	1000
Co60	Al	0.75	1000
Co60	Al	1	1000
Co60	Al	1.5	1000
Co60	Al	3	1000
Co60	Bare	0	1000
Co60	Pb	0.03125	1000
Co60	Pb	0.0625	1000
Co60	Pb	0.125	1000
Co60	Pb	0.25	1000
Co60	Pb	0.5	1000
Co60	Pb	1000	1000
Co60	Steel	0.125	1000
Co60	Steel	0.25	1000
Co60	Steel	0.5	1000
Co60	Steel	0.75	1000
Co60	Steel	10	1000
Co60	Steel	1.5	1000
Co60	Al	0.25	100
Co60	Al	0.5	100
Co60	Al	0.75	100
Co60	Al	1	100
Co60	Al	1.5	100
Co60	Al	3	100
Co60	Bare	0	100
Co60	Pb	0.03125	100
Co60	Pb	0.0625	100

Isotope	Shielding Material	Shielding Thickness (In)	Strength (μCi)
Co60	Pb	0.125	100
Co60	Pb	0.25	100
Co60	Pb	0.5	100
Co60	Pb	1000	100
Co60	Steel	0.125	100
Co60	Steel	0.25	100
Co60	Steel	0.5	100
Co60	Steel	0.75	100
Co60	Steel	10	100
Co60	Steel	1.5	100
Co60	Al	0.25	10
Co60	Al	0.5	10
Co60	Al	0.75	10
Co60	Al	1	10
Co60	Al	1.5	10
Co60	Al	3	10
Co60	Bare	0	10
Co60	Pb	0.03125	10
Co60	Pb	0.0625	10
Co60	Pb	0.125	10
Co60	Pb	0.25	10
Co60	Pb	0.5	10
Co60	Pb	1000	10
Co60	Steel	0.125	10
Co60	Steel	0.25	10
Co60	Steel	0.5	10
Co60	Steel	0.75	10
Co60	Steel	10	10
Co60	Steel	1.5	10
Co60	Al	0.25	200
Co60	Al	0.5	200
Co60	Al	0.75	200
Co60	Al	1	200
Co60	Al	1.5	200
Co60	Al	3	200
Co60	Bare	0	200
Co60	Pb	0.03125	200
Co60	Pb	0.0625	200
Co60	Pb	0.125	200
Co60	Pb	0.25	200

Isotope	Shielding Material	Shielding Thickness (In)	Strength (μCi)
Co60	Pb	0.5	200
Co60	Pb	1000	200
Co60	Steel	0.125	200
Co60	Steel	0.25	200
Co60	Steel	0.5	200
Co60	Steel	0.75	200
Co60	Steel	10	200
Co60	Steel	1.5	200
Co60	Al	0.25	350
Co60	Al	0.5	350
Co60	Al	0.75	350
Co60	Al	1	350
Co60	Al	1.5	350
Co60	Al	3	350
Co60	Bare	0	350
Co60	Pb	0.03125	350
Co60	Pb	0.0625	350
Co60	Pb	0.125	350
Co60	Pb	0.25	350
Co60	Pb	0.5	350
Co60	Pb	1000	350
Co60	Steel	0.125	350
Co60	Steel	0.25	350
Co60	Steel	0.5	350
Co60	Steel	0.75	350
Co60	Steel	10	350
Co60	Steel	1.5	350
Co60	Al	0.25	500
Co60	Al	0.5	500
Co60	Al	0.75	500
Co60	Al	1	500
Co60	Al	1.5	500
Co60	Al	3	500
Co60	Bare	0	500
Co60	Pb	0.03125	500
Co60	Pb	0.0625	500
Co60	Pb	0.125	500
Co60	Pb	0.25	500
Co60	Pb	0.5	500
Co60	Pb	1000	500

Isotope	Shielding Material	Shielding Thickness (In)	Strength (μCi)
Co60	Steel	0.125	500
Co60	Steel	0.25	500
Co60	Steel	0.5	500
Co60	Steel	0.75	500
Co60	Steel	10	500
Co60	Steel	1.5	500
Co60	Al	0.25	750
Co60	Al	0.5	750
Co60	Al	0.75	750
Co60	Al	1	750
Co60	Al	1.5	750
Co60	Al	3	750
Co60	Bare	0	750
Co60	Pb	0.03125	750
Co60	Pb	0.0625	750
Co60	Pb	0.125	750
Co60	Pb	0.25	750
Co60	Pb	0.5	750
Co60	Pb	1000	750
Co60	Steel	0.125	750
Co60	Steel	0.25	750
Co60	Steel	0.5	750
Co60	Steel	0.75	750
Co60	Steel	10	750
Co60	Steel	1.5	750
Cs137	Al	0.25	1000
Cs137	Al	0.5	1000
Cs137	Al	0.75	1000
Cs137	Al	1	1000
Cs137	Al	1.5	1000
Cs137	Al	3	1000
Cs137	Bare	0	1000
Cs137	Pb	0.03125	1000
Cs137	Pb	0.0625	1000
Cs137	Pb	0.125	1000
Cs137	Pb	0.25	1000
Cs137	Pb	0.5	1000
Cs137	Pb	1000	1000
Cs137	Steel	0.125	1000
Cs137	Steel	0.25	1000

Isotope	Shielding Material	Shielding Thickness (In)	Strength (μCi)
Cs137	Steel	0.5	1000
Cs137	Steel	0.75	1000
Cs137	Steel	10	1000
Cs137	Steel	1.5	1000
Cs137	Al	0.25	100
Cs137	Al	0.5	100
Cs137	Al	0.75	100
Cs137	Al	1	100
Cs137	Al	1.5	100
Cs137	Al	3	100
Cs137	Bare	0	100
Cs137	Pb	0.03125	100
Cs137	Pb	0.0625	100
Cs137	Pb	0.125	100
Cs137	Pb	0.25	100
Cs137	Pb	0.5	100
Cs137	Pb	1000	100
Cs137	Steel	0.125	100
Cs137	Steel	0.25	100
Cs137	Steel	0.5	100
Cs137	Steel	0.75	100
Cs137	Steel	10	100
Cs137	Steel	1.5	100
Cs137	Al	0.25	10
Cs137	Al	0.5	10
Cs137	Al	0.75	10
Cs137	Al	1	10
Cs137	Al	1.5	10
Cs137	Al	3	10
Cs137	Bare	0	10
Cs137	Pb	0.03125	10
Cs137	Pb	0.0625	10
Cs137	Pb	0.125	10
Cs137	Pb	0.25	10
Cs137	Pb	0.5	10
Cs137	Pb	1000	10
Cs137	Steel	0.125	10
Cs137	Steel	0.25	10
Cs137	Steel	0.5	10
Cs137	Steel	0.75	10

Isotope	Shielding Material	Shielding Thickness (In)	Strength (μCi)
Cs137	Steel	10	10
Cs137	Steel	1.5	10
Cs137	Al	0.25	200
Cs137	Al	0.5	200
Cs137	Al	0.75	200
Cs137	Al	1	200
Cs137	Al	1.5	200
Cs137	Al	3	200
Cs137	Bare	0	200
Cs137	Pb	0.03125	200
Cs137	Pb	0.0625	200
Cs137	Pb	0.125	200
Cs137	Pb	0.25	200
Cs137	Pb	0.5	200
Cs137	Pb	1000	200
Cs137	Steel	0.125	200
Cs137	Steel	0.25	200
Cs137	Steel	0.5	200
Cs137	Steel	0.75	200
Cs137	Steel	10	200
Cs137	Steel	1.5	200
Cs137	Al	0.25	350
Cs137	Al	0.5	350
Cs137	Al	0.75	350
Cs137	Al	1	350
Cs137	Al	1.5	350
Cs137	Al	3	350
Cs137	Bare	0	350
Cs137	Pb	0.03125	350
Cs137	Pb	0.0625	350
Cs137	Pb	0.125	350
Cs137	Pb	0.25	350
Cs137	Pb	0.5	350
Cs137	Pb	1000	350
Cs137	Steel	0.125	350
Cs137	Steel	0.25	350
Cs137	Steel	0.5	350
Cs137	Steel	0.75	350
Cs137	Steel	10	350
Cs137	Steel	1.5	350

Isotope	Shielding Material	Shielding Thickness (In)	Strength (μCi)
Cs137	Al	0.25	500
Cs137	Al	0.5	500
Cs137	Al	0.75	500
Cs137	Al	1	500
Cs137	Al	1.5	500
Cs137	Al	3	500
Cs137	Bare	0	500
Cs137	Pb	0.03125	500
Cs137	Pb	0.0625	500
Cs137	Pb	0.125	500
Cs137	Pb	0.25	500
Cs137	Pb	0.5	500
Cs137	Pb	1000	500
Cs137	Steel	0.125	500
Cs137	Steel	0.25	500
Cs137	Steel	0.5	500
Cs137	Steel	0.75	500
Cs137	Steel	10	500
Cs137	Steel	1.5	500
Cs137	Al	0.25	750
Cs137	Al	0.5	750
Cs137	Al	0.75	750
Cs137	Al	1	750
Cs137	Al	1.5	750
Cs137	Al	3	750
Cs137	Bare	0	750
Cs137	Pb	0.03125	750
Cs137	Pb	0.0625	750
Cs137	Pb	0.125	750
Cs137	Pb	0.25	750
Cs137	Pb	0.5	750
Cs137	Pb	1000	750
Cs137	Steel	0.125	750
Cs137	Steel	0.25	750
Cs137	Steel	0.5	750
Cs137	Steel	0.75	750
Cs137	Steel	10	750
Cs137	Steel	1.5	750
Mn54	Al	0.25	1000
Mn54	Al	0.5	1000

Isotope	Shielding Material	Shielding Thickness (In)	Strength (μCi)
Mn54	Al	0.75	1000
Mn54	Al	1	1000
Mn54	Al	1.5	1000
Mn54	Al	3	1000
Mn54	Bare	0	1000
Mn54	Pb	0.03125	1000
Mn54	Pb	0.0625	1000
Mn54	Pb	0.125	1000
Mn54	Pb	0.25	1000
Mn54	Pb	0.5	1000
Mn54	Pb	1000	1000
Mn54	Steel	0.125	1000
Mn54	Steel	0.25	1000
Mn54	Steel	0.5	1000
Mn54	Steel	0.75	1000
Mn54	Steel	10	1000
Mn54	Steel	1.5	1000
Mn54	Al	0.25	100
Mn54	Al	0.5	100
Mn54	Al	0.75	100
Mn54	Al	1	100
Mn54	Al	1.5	100
Mn54	Al	3	100
Mn54	Bare	0	100
Mn54	Pb	0.03125	100
Mn54	Pb	0.0625	100
Mn54	Pb	0.125	100
Mn54	Pb	0.25	100
Mn54	Pb	0.5	100
Mn54	Pb	1000	100
Mn54	Steel	0.125	100
Mn54	Steel	0.25	100
Mn54	Steel	0.5	100
Mn54	Steel	0.75	100
Mn54	Steel	10	100
Mn54	Steel	1.5	100
Mn54	Al	0.25	10
Mn54	Al	0.5	10
Mn54	Al	0.75	10
Mn54	Al	1	10

Isotope	Shielding Material	Shielding Thickness (In)	Strength (μCi)
Mn54	Al	1.5	10
Mn54	Al	3	10
Mn54	Bare	0	10
Mn54	Pb	0.03125	10
Mn54	Pb	0.0625	10
Mn54	Pb	0.125	10
Mn54	Pb	0.25	10
Mn54	Pb	0.5	10
Mn54	Pb	1000	10
Mn54	Steel	0.125	10
Mn54	Steel	0.25	10
Mn54	Steel	0.5	10
Mn54	Steel	0.75	10
Mn54	Steel	10	10
Mn54	Steel	1.5	10
Mn54	Al	0.25	200
Mn54	Al	0.5	200
Mn54	Al	0.75	200
Mn54	Al	1	200
Mn54	Al	1.5	200
Mn54	Al	3	200
Mn54	Bare	0	200
Mn54	Pb	0.03125	200
Mn54	Pb	0.0625	200
Mn54	Pb	0.125	200
Mn54	Pb	0.25	200
Mn54	Pb	0.5	200
Mn54	Pb	1000	200
Mn54	Steel	0.125	200
Mn54	Steel	0.25	200
Mn54	Steel	0.5	200
Mn54	Steel	0.75	200
Mn54	Steel	10	200
Mn54	Steel	1.5	200
Mn54	Al	0.25	350
Mn54	Al	0.5	350
Mn54	Al	0.75	350
Mn54	Al	1	350
Mn54	Al	1.5	350
Mn54	Al	3	350

Isotope	Shielding Material	Shielding Thickness (In)	Strength (μCi)
Mn54	Bare	0	350
Mn54	Pb	0.03125	350
Mn54	Pb	0.0625	350
Mn54	Pb	0.125	350
Mn54	Pb	0.25	350
Mn54	Pb	0.5	350
Mn54	Pb	1000	350
Mn54	Steel	0.125	350
Mn54	Steel	0.25	350
Mn54	Steel	0.5	350
Mn54	Steel	0.75	350
Mn54	Steel	10	350
Mn54	Steel	1.5	350
Mn54	Al	0.25	500
Mn54	Al	0.5	500
Mn54	Al	0.75	500
Mn54	Al	1	500
Mn54	Al	1.5	500
Mn54	Al	3	500
Mn54	Bare	0	500
Mn54	Pb	0.03125	500
Mn54	Pb	0.0625	500
Mn54	Pb	0.125	500
Mn54	Pb	0.25	500
Mn54	Pb	0.5	500
Mn54	Pb	1000	500
Mn54	Steel	0.125	500
Mn54	Steel	0.25	500
Mn54	Steel	0.5	500
Mn54	Steel	0.75	500
Mn54	Steel	10	500
Mn54	Steel	1.5	500
Mn54	Al	0.25	750
Mn54	Al	0.5	750
Mn54	Al	0.75	750
Mn54	Al	1	750
Mn54	Al	1.5	750
Mn54	Al	3	750
Mn54	Bare	0	750
Mn54	Pb	0.03125	750

Isotope	Shielding Material	Shielding Thickness (In)	Strength (μCi)
Mn54	Pb	0.0625	750
Mn54	Pb	0.125	750
Mn54	Pb	0.25	750
Mn54	Pb	0.5	750
Mn54	Pb	1000	750
Mn54	Steel	0.125	750
Mn54	Steel	0.25	750
Mn54	Steel	0.5	750
Mn54	Steel	0.75	750
Mn54	Steel	10	750
Mn54	Steel	1.5	750
Na22	Al	0.25	1000
Na22	Al	0.5	1000
Na22	Al	0.75	1000
Na22	Al	1	1000
Na22	Al	1.5	1000
Na22	Al	3	1000
Na22	Bare	0	1000
Na22	Pb	0.03125	1000
Na22	Pb	0.0625	1000
Na22	Pb	0.125	1000
Na22	Pb	0.25	1000
Na22	Pb	0.5	1000
Na22	Pb	1000	1000
Na22	Steel	0.125	1000
Na22	Steel	0.25	1000
Na22	Steel	0.5	1000
Na22	Steel	0.75	1000
Na22	Steel	10	1000
Na22	Steel	1.5	1000
Na22	Al	0.25	100
Na22	Al	0.5	100
Na22	Al	0.75	100
Na22	Al	1	100
Na22	Al	1.5	100
Na22	Al	3	100
Na22	Bare	0	100
Na22	Pb	0.03125	100
Na22	Pb	0.0625	100
Na22	Pb	0.125	100

Isotope	Shielding Material	Shielding Thickness (In)	Strength (μCi)
Na22	Pb	0.25	100
Na22	Pb	0.5	100
Na22	Pb	1000	100
Na22	Steel	0.125	100
Na22	Steel	0.25	100
Na22	Steel	0.5	100
Na22	Steel	0.75	100
Na22	Steel	10	100
Na22	Steel	1.5	100
Na22	Al	0.25	10
Na22	Al	0.5	10
Na22	Al	0.75	10
Na22	Al	1	10
Na22	Al	1.5	10
Na22	Al	3	10
Na22	Bare	0	10
Na22	Pb	0.03125	10
Na22	Pb	0.0625	10
Na22	Pb	0.125	10
Na22	Pb	0.25	10
Na22	Pb	0.5	10
Na22	Pb	1000	10
Na22	Steel	0.125	10
Na22	Steel	0.25	10
Na22	Steel	0.5	10
Na22	Steel	0.75	10
Na22	Steel	10	10
Na22	Steel	1.5	10
Na22	Al	0.25	200
Na22	Al	0.5	200
Na22	Al	0.75	200
Na22	Al	1	200
Na22	Al	1.5	200
Na22	Al	3	200
Na22	Bare	0	200
Na22	Pb	0.03125	200
Na22	Pb	0.0625	200
Na22	Pb	0.125	200
Na22	Pb	0.25	200
Na22	Pb	0.5	200

Isotope	Shielding Material	Shielding Thickness (In)	Strength (μCi)
Na22	Pb	1000	200
Na22	Steel	0.125	200
Na22	Steel	0.25	200
Na22	Steel	0.5	200
Na22	Steel	0.75	200
Na22	Steel	10	200
Na22	Steel	1.5	200
Na22	Al	0.25	350
Na22	Al	0.5	350
Na22	Al	0.75	350
Na22	Al	1	350
Na22	Al	1.5	350
Na22	Al	3	350
Na22	Bare	0	350
Na22	Pb	0.03125	350
Na22	Pb	0.0625	350
Na22	Pb	0.125	350
Na22	Pb	0.25	350
Na22	Pb	0.5	350
Na22	Pb	1000	350
Na22	Steel	0.125	350
Na22	Steel	0.25	350
Na22	Steel	0.5	350
Na22	Steel	0.75	350
Na22	Steel	10	350
Na22	Steel	1.5	350
Na22	Al	0.25	500
Na22	Al	0.5	500
Na22	Al	0.75	500
Na22	Al	1	500
Na22	Al	1.5	500
Na22	Al	3	500
Na22	Bare	0	500
Na22	Pb	0.03125	500
Na22	Pb	0.0625	500
Na22	Pb	0.125	500
Na22	Pb	0.25	500
Na22	Pb	0.5	500
Na22	Pb	1000	500
Na22	Steel	0.125	500

Isotope	Shielding Material	Shielding Thickness (In)	Strength (μCi)
Na22	Steel	0.25	500
Na22	Steel	0.5	500
Na22	Steel	0.75	500
Na22	Steel	10	500
Na22	Steel	1.5	500
Na22	Al	0.25	750
Na22	Al	0.5	750
Na22	Al	0.75	750
Na22	Al	1	750
Na22	Al	1.5	750
Na22	Al	3	750
Na22	Bare	0	750
Na22	Pb	0.03125	750
Na22	Pb	0.0625	750
Na22	Pb	0.125	750
Na22	Pb	0.25	750
Na22	Pb	0.5	750
Na22	Pb	1000	750
Na22	Steel	0.125	750
Na22	Steel	0.25	750
Na22	Steel	0.5	750
Na22	Steel	0.75	750
Na22	Steel	10	750
Na22	Steel	1.5	750
Ra226	Al	0.25	1000
Ra226	Al	0.5	1000
Ra226	Al	0.75	1000
Ra226	Al	1	1000
Ra226	Al	1.5	1000
Ra226	Al	3	1000
Ra226	Bare	0	1000
Ra226	Pb	0.03125	1000
Ra226	Pb	0.0625	1000
Ra226	Pb	0.125	1000
Ra226	Pb	0.25	1000
Ra226	Pb	0.5	1000
Ra226	Pb	1000	1000
Ra226	Steel	0.125	1000
Ra226	Steel	0.25	1000
Ra226	Steel	0.5	1000

Isotope	Shielding Material	Shielding Thickness (In)	Strength (μCi)
Ra226	Steel	0.75	1000
Ra226	Steel	10	1000
Ra226	Steel	1.5	1000
Ra226	Al	0.25	100
Ra226	Al	0.5	100
Ra226	Al	0.75	100
Ra226	Al	1	100
Ra226	Al	1.5	100
Ra226	Al	3	100
Ra226	Bare	0	100
Ra226	Pb	0.03125	100
Ra226	Pb	0.0625	100
Ra226	Pb	0.125	100
Ra226	Pb	0.25	100
Ra226	Pb	0.5	100
Ra226	Pb	1000	100
Ra226	Steel	0.125	100
Ra226	Steel	0.25	100
Ra226	Steel	0.5	100
Ra226	Steel	0.75	100
Ra226	Steel	10	100
Ra226	Steel	1.5	100
Ra226	Al	0.25	10
Ra226	Al	0.5	10
Ra226	Al	0.75	10
Ra226	Al	1	10
Ra226	Al	1.5	10
Ra226	Al	3	10
Ra226	Bare	0	10
Ra226	Pb	0.03125	10
Ra226	Pb	0.0625	10
Ra226	Pb	0.125	10
Ra226	Pb	0.25	10
Ra226	Pb	0.5	10
Ra226	Pb	1000	10
Ra226	Steel	0.125	10
Ra226	Steel	0.25	10
Ra226	Steel	0.5	10
Ra226	Steel	0.75	10
Ra226	Steel	10	10

Isotope	Shielding Material	Shielding Thickness (In)	Strength (μCi)
Ra226	Steel	1.5	10
Ra226	Al	0.25	200
Ra226	Al	0.5	200
Ra226	Al	0.75	200
Ra226	Al	1	200
Ra226	Al	1.5	200
Ra226	Al	3	200
Ra226	Bare	0	200
Ra226	Pb	0.03125	200
Ra226	Pb	0.0625	200
Ra226	Pb	0.125	200
Ra226	Pb	0.25	200
Ra226	Pb	0.5	200
Ra226	Pb	1000	200
Ra226	Steel	0.125	200
Ra226	Steel	0.25	200
Ra226	Steel	0.5	200
Ra226	Steel	0.75	200
Ra226	Steel	10	200
Ra226	Steel	1.5	200
Ra226	Al	0.25	350
Ra226	Al	0.5	350
Ra226	Al	0.75	350
Ra226	Al	1	350
Ra226	Al	1.5	350
Ra226	Al	3	350
Ra226	Bare	0	350
Ra226	Pb	0.03125	350
Ra226	Pb	0.0625	350
Ra226	Pb	0.125	350
Ra226	Pb	0.25	350
Ra226	Pb	0.5	350
Ra226	Pb	1000	350
Ra226	Steel	0.125	350
Ra226	Steel	0.25	350
Ra226	Steel	0.5	350
Ra226	Steel	0.75	350
Ra226	Steel	10	350
Ra226	Steel	1.5	350
Ra226	Al	0.25	500

Isotope	Shielding Material	Shielding Thickness (In)	Strength (μCi)
Ra226	Al	0.5	500
Ra226	Al	0.75	500
Ra226	Al	1	500
Ra226	Al	1.5	500
Ra226	Al	3	500
Ra226	Bare	0	500
Ra226	Pb	0.03125	500
Ra226	Pb	0.0625	500
Ra226	Pb	0.125	500
Ra226	Pb	0.25	500
Ra226	Pb	0.5	500
Ra226	Pb	1000	500
Ra226	Steel	0.125	500
Ra226	Steel	0.25	500
Ra226	Steel	0.5	500
Ra226	Steel	0.75	500
Ra226	Steel	10	500
Ra226	Steel	1.5	500
Ra226	Al	0.25	750
Ra226	Al	0.5	750
Ra226	Al	0.75	750
Ra226	Al	1	750
Ra226	Al	1.5	750
Ra226	Al	3	750
Ra226	Bare	0	750
Ra226	Pb	0.03125	750
Ra226	Pb	0.0625	750
Ra226	Pb	0.125	750
Ra226	Pb	0.25	750
Ra226	Pb	0.5	750
Ra226	Pb	1000	750
Ra226	Steel	0.125	750
Ra226	Steel	0.25	750
Ra226	Steel	0.5	750
Ra226	Steel	0.75	750
Ra226	Steel	10	750
Ra226	Steel	1.5	750

DISTRIBUTION

Email—Internal

Name	Org.	Sandia Email Address
Jay Brotz	6831	jkbrotz@sandia.gov
Eduardo Padilla	6831	eapadil@sandia.gov
Jesus Valencia	6831	jjvale@sandia.gov
Michael Higgins	6832	mhiggin@sandia.gov
Technical Library	01177	libref@sandia.gov

Email—External (encrypt for OUO)

Name	Company Email Address	Company Name
John Dunn	john.dunn@nnsa.doe.gov	DOE NA-243

Sandia National Laboratories

Sandia National Laboratories is a multimission laboratory managed and operated by National Technology & Engineering Solutions of Sandia LLC, a wholly owned subsidiary of Honeywell International Inc. for the U.S. Department of Energy's National Nuclear Security Administration under contract DE-NA0003525.